

LA-4631-MS

N71-20373

NASH CR-117315

LOS ALAMOS SCIENTIFIC LABORATORY
of the
University of California
LOS ALAMOS • NEW MEXICO

CASE FILE
COPY

CMF-13 Research on Carbon and Graphite

Report No. 15

Summary of Progress from August 1 to October 31, 1970

This report was prepared as an account of work sponsored by the United States Government. Neither the United States nor the United States Atomic Energy Commission, nor any of their employees, nor any of their contractors, subcontractors, or their employees, makes any warranty, express or implied, or assumes any legal liability or responsibility for the accuracy, completeness or usefulness of any information, apparatus, product or process disclosed, or represents that its use would not infringe privately owned rights.

This LA. . MS report presents the summary of progress of CMF-13 research on carbon and graphite at LASL. The four most recent Summary of Progress Reports in this series, all unclassified, are:

LA-4333-MS
LA-4417-MS

LA-4480-MS
LA-4526-MS

This report, like other special-purpose documents in the LA. . MS series, has not been reviewed or verified for accuracy in the interest of prompt distribution.

Distributed: February 1971

LA-4631-MS
SPECIAL DISTRIBUTION

LOS ALAMOS SCIENTIFIC LABORATORY
of the
University of California
LOS ALAMOS • NEW MEXICO

CMF-13 Research on Carbon and Graphite

Report No. 15

Summary of Progress from August 1 to October 31, 1970*

by

Morton C. Smith

*Supported in part by the Office of Advanced Research and Technology of the National Aeronautics and Space Administration.

CMF-13 RESEARCH ON CARBON AND GRAPHITE

REPORT NO. 15: SUMMARY OF PROGRESS FROM AUGUST 1 TO OCTOBER 31, 1970

by

Morton C. Smith

I. INTRODUCTION

This is the fifteenth in a series of progress reports devoted to carbon and graphite research in LASL Group CMF-13, and summarizes work done during the months of August, September, and October, 1970. It should be understood that in such a progress report many of the data are preliminary, incomplete, and subject to correction, and many of the opinions and conclusions are tentative and subject to change. This report is intended only to provide up-to-date background information to those who are interested in the materials and programs described in it, and should not be quoted or used as a reference publicly or in print.

Research and development on carbon and graphite were undertaken by CMF-13 primarily to increase understanding of their properties and behavior as engineering materials, to improve the raw materials and processes used in their manufacture, and to learn how to produce them with consistent, predictable, useful combinations of properties. The approach taken is microstructural, based on study and characterization of natural, commercial, and experimental carbons and graphites by such techniques as x-ray diffraction, electron and optical microscopy, and porosimetry. Physical and mechanical properties are measured as functions of formulation, treatment, and environmental variables, and correlations are sought among properties and structures. Raw materials and manufacturing techniques are investigated, improved, and varied systematically in an effort to create specific internal structures believed to be responsible

for desirable combinations of properties. Prompt feedback of information among these activities then makes possible progress in all of them toward their common goal of understanding and improving manufactured carbons and graphites.

Since its beginning, this research has been sponsored by the Division of Space Nuclear Systems of the United States Atomic Energy Commission, through the Space Nuclear Propulsion Office. More recently additional general support for it has been provided by the Office of Advanced Research and Technology of the National Aeronautics and Space Administration. Many of its facilities and services have been furnished by the Division of Military Application of AEC. The direct and indirect support and the guidance and encouragement of these agencies of the United States Government are gratefully acknowledged.

II. SANTA MARIA COKE

A. Previous Work

Investigations of Santa Maria coke and of graphites made from it have previously been discussed in Reports 9 through 14 in this series.

B. Santa Maria Fillers (R. J. Imprescia)

Santa Maria graphite flour, CMF-13 Lot G-26, has been used as the principal filler material in the manufacture of a large number of both molded and extruded experimental graphites. It was obtained from the Y-12 Plant of Union Carbide Corporation, who prepared it by grinding calcined Santa Maria LV coke, graphitizing the

TABLE I
SIEVE ANALYSES OF SANTA MARIA FILLERS (Y-12 BLEND NO. 1)

Fraction (U.S. Std. Series)	Weight Percent in Screen Fraction				
	Lot G-26 (Screened)	Lot G-35		Lot C-15	
		Unscreened	Screened	Unscreened	Screened
+ 16	0	trace	0	0	0
-16 + 25	0	0.7	0	trace	0
-25 + 45	trace	0.8	0	2.0	0
-45 + 80	3.8	3.5	2.5	1.5	3.0
-80 + 170	19.6	10.0	12.5	12.5	15.0
-170 + 325	21.2	18.5	17.5	20.0	19.0
-325	55.4	66.5	67.5	64.0	63.0

ground product at 2500°C, then screening the graphite flour to remove plus 60-mesh oversize. It was identified by Y-12 as "Santa Maria Blend No. 1."

Recently, two new lots of the "Blend No. 1" grind have been received from Y-12. One of these, CMF-13 Lot C-15, was in the calcined (LV) condition, unscreened; the other, CMF-13 Lot G-35, had been graphitized at Y-12 to 2500°C, and was also unscreened. Samples of the two lots were screened by CMF-13 on a SWECO Vibro-Energy Separator to remove plus 62 mesh oversize (which is nominally plus 50 mesh in the U.S. Standard Screen Series), and were subjected to sieve analysis. Sieve analyses were also made on unscreened samples. These analyses are compared with each other and with that of the previous Lot G-26 in Table I. It is apparent that the two new lots are quite similar to each other, and distinctly different from the older lot. In particular, Lot G-35, after screening, is a much finer product than is Lot G-26, which it was expected to duplicate.

Additional data on Lots C-15 and G-26 are given below in Tables V and VI and Fig. 2.

C. Molded Resin-Bonded Graphites (R. J. Imprescia)

Manufacturing and density data for the Series 63 hot-molded graphites were given in Report 13 in this series, pages 8-9. All were made using Santa Maria graphite flour, CMF-13 Lot G-26, with 20 pph of an experimental, high-viscosity, furfuryl alcohol resin binder, EMW-1600. The properties of two additional members of this series, Specimens 63V-1 and 63W-1, are listed in Table II.

These two graphites differed only in the proportion of maleic anhydride curing catalyst added to the binder, which was 1.0% for Specimen 63V-1 and only 0.5% for 63W-1. They were very similar in microstructure, having fine ($< 5 \mu$ dia), uniformly distributed pores, and no gross defects. However, Specimen 63V-1 (which had the greater catalyst concentration) contained microcracks up to about 100μ long between some of the larger filler particles, while none were observed in 63W-1. The microcracks had no large effect on properties, but were preferentially oriented normal to the molding axis and were probably responsible for the slightly greater anisotropy of properties -- particularly of compressive strength and electrical resistivity -- of Specimen 63V-1.

Use of the smaller proportion of curing catalyst appears to be desirable.

D. Molded Pitch-Bonded Graphites (R. J. Imprescia)

The Series 64 graphites listed in Table II were made from Santa Maria LV coke (calcined by its manufacturer to about 1090°C), ground to various degrees of fineness, and were hot-molded using Barrett 30MH coal-tar pitch binder. Microstructurally, all specimens were quite similar. All appeared to be deficient in fines, and the binder residue was difficult to identify. Pores were generally irregular in shape. In Specimen 64H-2, molded at only 500 psi, the pores occurred mostly in clusters of fines between large filler particles. Specimen 64I-1, molded at 4000 psi and with perhaps the best properties of any graphite in this series, had an unusual microstruc-

TABLE II

PROPERTIES OF SOME MOLDED SANTA MARIA GRAPHITES

SPECIMEN NO.:	63V-1	63W-1	64G-1	64H-1	64H-3	64H-2	64 I-1	64J-1
Filler Fines, % -325#	---	---	19.0	28.0	28.0	28.0	32.5	31.5
Molding Pressure, psi	4000	4000	4000	4000	2000	500	4000	4000
Density, g/cm ³	1.780	1.798	1.790	1.796	1.765	1.647	1.774	1.755
Tensile Str., psi								
With-grain	---	---	3683	3484 ^(c)	4021	1634	4118	3731
Compr. Str., psi								
With-grain	13,860	11,226	---	---	13,887	7067	14,886	13,623
Across-grain	10,803	11,165	---	---	14,162	6870	14,231	13,610
Flexure Str., psi								
With-grain	---	---	5737	5759	6257	2390	6391	5480
Across-grain	---	---	6014	5892	5874	1947	6307	5656
CTE, x 10 ⁻⁶ /°C ^(a)								
With-grain	5.83	5.24	5.01	5.19	5.56	5.29	5.72	6.36
Across-grain	6.54	5.74	5.46	5.72	6.02	5.58	6.42	6.09
Resistivity, μΩ cm								
With-grain	1509	1421	1285	1285	1329	1935	1320	1321
Across-grain	1728	1529	1261	1290	1367	2035	1361	1353
Therm. Cond., W/cm-°C								
With-grain	0.70	0.80	1.10	1.10	0.91	0.57	1.01	1.00
Across-grain	0.68	0.76	1.06	1.10	0.88	0.63	0.98	0.97
Young's Mod., 10 ⁶ psi								
With-grain	1.35	1.34	---	---	1.42	0.813	1.44	1.38
Across-grain	1.31	1.18	---	---	1.41	0.790	1.43	1.36
Anisotropies								
BAF ^(b)	1.033	1.039	1.006	1.022	1.013	1.033	1.025	1.019
Compr. Str.	0.78	0.99	---	---	1.02	0.97	0.96	1.00
Flexure Str.	---	---	0.95	1.02	0.94	0.81	0.99	1.03
CTE	1.12	1.10	1.09	1.10	1.08	1.05	1.12	0.96
Resistivity	1.15	1.08	0.98	1.00	1.03	1.05	1.03	1.02
Therm. Cond.	1.03	1.05	1.04	1.00	1.03	0.90	1.03	1.03
Young's Mod.	1.03	1.14	---	---	1.01	1.03	1.01	1.01

(a) Coefficient of thermal expansion, average 25-645°C

(b) Bacon Anisotropy Factor, σ_{oz}/σ_{ox}

(c) Specimen broke outside gauge section

tural characteristic: a very spongy network of fines plus binder residue in the interstices between the larger filler particles.

Considering only the Series 64 graphites molded at 4000 psi, it appears that increasing the filler fineness (percent minus 325 mesh) resulted in small increases in strength properties and small decreases in thermal conductivity. However, the properties of all of these graphites were much alike.

Decreasing the molding pressure from 4000 to 2000 psi had little effect on structure or properties. A further

decrease to 500 psi reduced most properties significantly.

Except for the specimen molded at 500 psi, all of the Series 64 graphites had good properties. They were generally less anisotropic than were the resin-bonded graphites of Series 63, and had slightly higher strengths, Young's moduli, and thermal and electrical conductivities. Thermal expansion coefficients were similar for the two types of graphite and, in the pitch-bonded series, increased with increasing fineness of the filler.

TABLE III
PROPERTIES OF HOT-MOLDED, RESIN-BONDED, SANTA MARIA GRAPHITES

<u>SPECIMEN NO.:</u>	<u>70C-1b^(a)</u>	<u>70B-1^(a)</u>	<u>70A-1^(a)</u>	<u>70D-2</u>
Extrusion Mix No.	ACS-4	ACS-2, 3	ACS-1	ACS-5
Binder Viscosity, cp	10	250	255	1400
Bulk Density, g/cm ³				
Baked Condition	1.811	---	1.778	1.761
Graphitized	1.880	1.803	1.816	1.785
Dimensional Change, Baked to Graphitized Condition, %				
Δl	-0.9	---	-0.6	-0.2
Δd	-1.6	-0.9	-0.9	-0.7
Δv	-4.1	---	-2.4	-1.6
Flexure Strength, psi				
With-grain	3512	2514	4340 ^(b)	2775
Across-grain	1643	565	281 ^(b)	2714
CTE (Ave., 25-645°C), $\times 10^{-6}/^{\circ}\text{C}$				
With-grain	5.11	5.12	5.44	6.07
Across-grain	4.54	6.00	5.86	6.04
Resistivity, $\mu\Omega\text{cm}$				
With-grain	2640	1835	1793	1894
Across-grain	2683	3149	1927	1982
Young's Modulus, 10^6 psi				
With-grain	1.404	1.557	1.533	1.165
Across-grain	1.378	1.237	1.095	1.355
Anisotropies				
BAF ^(c)	1.038	1.030	1.032	1.020
Flexure Strength	2.14	4.45	15.44	1.02
CTE	0.89	1.17	1.08	1.00
Resistivity	1.02	1.72	1.07	1.05
Young's Modulus	1.02	1.26	1.40	0.86

(a) Specimen cracked

(b) One specimen only

(c) Bacon Anisotropy Factor, σ_{oz}/σ_{ox}

E. Effects of Resin-Binder Viscosity (R. J. Imprescia)

Four hot-molded graphite specimens, listed in Table III, have been made from resin-bonded mixes originally prepared for extrusion experiments. The filler was 85 parts of CMF-13 Lot G-26 Santa Maria graphite flour, plus 15 parts of Thermax carbon black. The binder was an experimental furfuryl alcohol resin, EMW 1400, having a viscosity of about 1400 cp, to which -- in three of the four mixes -- furfuryl alcohol monomer was added to reduce its viscosity.

Three of the specimens were hot-molded by the

standard "Program A" and then graphitized in flowing argon to about 2800°C. Mix ACS-4, made from a very low-viscosity (10 cp) binder, exploded the graphite die, probably because of rapid evolution of a large volume of volatile material in the early stages of the hot-molding cycle. It was therefore compacted at 4000 psi at room temperature, cured in air at 75°C for 1 week, and then replaced in the die and hot-molded according to "Program A." Specimen 70C-1b, produced in this way, cracked during hot-molding, as did Specimens 70B-1 and 70A-1, made from somewhat higher-viscosity binders. Only

Specimen 70D-1, made from the undiluted high-viscosity resin, appeared to be sound.

Optical and electron microscopy showed that all specimens except 70D-1 contained systems of cracks, ranging from moderate to severe. Specimen 70D-1 was sound, with only a few pores in the size range above 5μ and a few fine void colonies and interface cracks at the surfaces of filler particles. Specimen 70C-1b contained many void colonies and stringers and some large ($50\text{--}100\mu$ dia) pores. The degree of penetration by the epoxy mounting resin was greater than in other specimens in this series, indicating a higher degree of interconnectedness of the porosity.

Bulk density in both the baked and the graphitized conditions increased with decreasing binder viscosity, which was the opposite of the trend previously established with similar series of extruded graphites. This may be a result of improved lubrication between particles provided by the monomer additions which may be more important with the thicker sections and restricted material flow of a molding operation than it is in extrusion. The only property other than density which varied systematically was the coefficient of thermal expansion, which -- in spite of decreasing density -- increased with increasing binder viscosity.

Crystallographic anisotropy, as indicated by the Bacon Anisotropy Factor, was quite low for all specimens. Specimen 70D-2, made from the highest-viscosity resin, was also nearly isotropic in its physical and mechanical properties. Specimens made from the lower-viscosity resins were highly anisotropic in some of their properties, undoubtedly because of a preferred orientation of cracks normal to the axis of molding pressure. The large volumes of pyrolysis gases evolved from the lower-viscosity resins at least contributed to this extensive cracking.

Washer-shaped specimens of graphite 70D-1, a duplicate of sample 70D-2, were tested in thermal shock by C. R. King of LASL Group N-7 in an apparatus in which the outside rim of the specimen is heated rapidly by a 100 kW, 350 kHz induction heater while its inner bore is cooled by a water-cooled metal finger. Thermal shock

indices were 285/290 in the with-grain orientation and 277.5/280 across-grain, which are quite low.

F. Effects of Filler Heat-Treatment Temperature (R. J. Imprescia)

In report No. 14 in this series (pp 2-3), manufacturing and density data were given for Series 66 hot-molded graphites, which were made from a group of Santa Maria fillers that had been calcined at temperatures from 620 to 2808°C. These fillers were the products of an earlier experiment, described in Reports 11 and 12, in which the effects of prior heat-treatment on the grindability of lump Santa Maria coke were investigated. It was found that heat-treatment temperature had strong effects on grindability and on the particle-size distribution of the grinding product. Therefore, the fillers used to make the Series 66 graphites varied widely in particle-size distribution, and in packing behavior, as well as in the temperature to which the filler had been heat-treated. It was not possible to separate the effects of these variables on the properties of the finished graphites.

In an attempt to eliminate the variable of particle-size distribution, the Series 73 graphites, listed in Table IV, were produced, using the same procedures used to make Series 66. However, the fillers used in Series 73 were heat-treated after grinding. The first four graphites in the series were made from CMF-13 Lot C-15 Santa Maria flour, the recent lot of Y-12 "Blend No. 1" material discussed above. Specimen 73 C-1 was made from this flour in the as-received or "LV" condition, calcined by the manufacturer to about 1090°C. Specimens 73D-1, 73E-2, and 73F-1 were made from the same flour after it had been calcined to 1470, 1840, and 2170°C respectively. Specimen 73G-2 was made from the older Lot G-26 graphite flour, which had been given a post-grind heat-treatment at Y-12 to 2500°C, and was assumed to have the same particle size distribution as Lot C-15. As has been discussed above, this assumption was incorrect.

Micromerograph particle-size distributions for the fillers used to make the Series 66 graphites are shown in Fig. 1. Those heat-treated below 2000°C are seen to differ considerably. Fig. 2 shows similar data for the

TABLE IV

DENSITY PROPERTIES FOR SERIES 73 HOT-MOLDED, PITCH-BONDED, SANTA MARIA GRAPHITES

Specimen No.	Calcining Temp., °C	Binder Conc., pph	Calculated Optimum Binder, pph	Binder Residue, % (Baked)	Density, g/cm ³			Dimensional Change Baked to Graph., %		
					Packed Filler (Baked)	Bulk Baked	Graph.	Δt	Δd	Δv
73C-1 (a)	As-rec'd	26	22.6	57.8	1.467	1.687	1.788	-3.8	-3.5	-10.5
73D-1 (a, b)	1470	25	24.2	60.5	1.518	1.748	1.787	-1.0	-1.2	-3.4
73E-2	1840	24	20.5	59.1	1.569	1.792	1.805	-0.2	-0.6	-1.3
73F-1	2170	24	19.1	58.9	1.599	1.825	1.821	+0.3	-0.3	-0.4
73G-2	2500	23	18.4	61.0	1.618	1.844	1.820	+0.9	0.0	+0.3

(a) Specimens 73C-1 and 73D-1 were graphitized at 2720°C; all others at 2788°C

(b) Specimen cracked during molding into pie-shaped segments

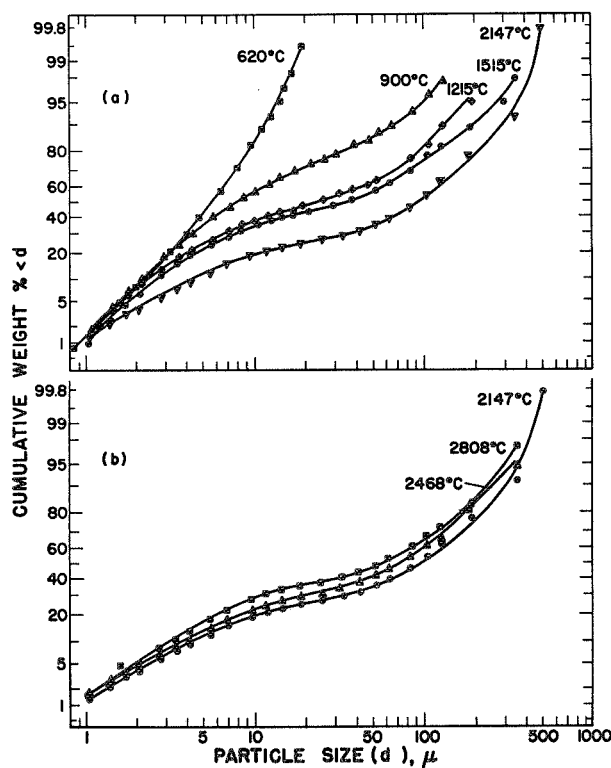


Fig. 1. Micromerograph particle-size data for Santa Maria fillers used to make Series 66 graphites. These fillers were heat-treated before they were ground, to the temperatures indicated in the figure.

fillers used to make Series 73. Obviously, these fillers are more nearly alike than are those which were heat-treated before grinding, but significant differences still

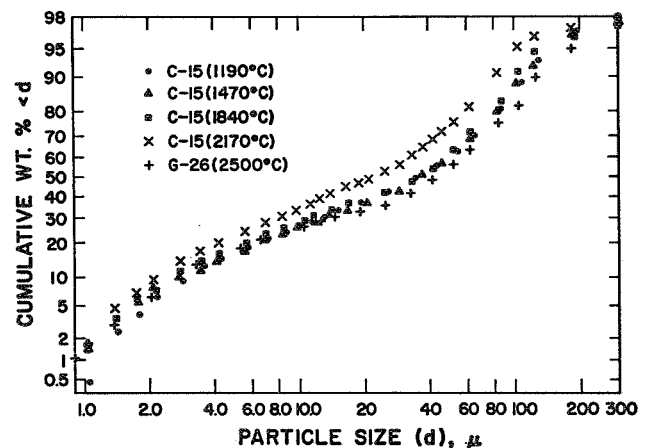


Fig. 2. Micromerograph particle-size data for Santa Maria fillers used to make Series 73 graphites. These fillers were heat-treated after they were ground, to the temperatures indicated in parentheses.

exist. These differences are emphasized by the helium-pycnometer densities, Micromerograph particle-size statistics, and surface-area data of Tables V and VI. As would be expected, heat-treating the ground LV coke to higher temperatures increased the particle density measured by helium pycnometry. However, the highest helium density resulted from calcination at 1470°C. (This was verified by three repeat determinations each on samples calcined at 1470 and 1840°C.) The 1470°C heat-treatment also resulted in the minimum mean particle diameter (\bar{d}), minimum variance (s_d^2), and maximum coefficient of var-

TABLE V
PARTICLE CHARACTERISTICS, HEAT-TREATED SANTA MARIA FILLERS

Filler		Helium Density, g/cm ³	Micromerograph Sample Statistics (Interval Model)							
Lot No.	Calcining Temp., °C		\bar{x}_3	s_x^2	\bar{x}	\bar{d}_3 Microns	\bar{d} , Microns	s_d^2 , Microns ²	S_W^2 , cm ² /g	CV_d
C-15	As-rec'd. ^(a)	1.955	3.232	0.189	0.360	55.00	1.626	1.447	3245	0.740
C-15	1470	2.096	3.238	0.155	0.111	55.40	1.256	0.877	3307	0.750
C-15	1840	2.071	3.153	0.165	0.165	53.10	1.328	0.921	3600	0.722
C-15	2170	2.075	2.833	0.160	0.190	41.13	1.355	0.891	4316	0.696
G-26	2500 ^(b)	2.084	3.317	0.177	0.218	57.55	1.410	1.050	3181	0.730

(a) Calcined by manufacturer at approximately 1090°C

(b) Graphitized at Y-12 Plant, Union Carbide Corporation

TABLE VI
SURFACE-AREA DATA, HEAT-TREATED SANTA MARIA FILLERS

Filler		S_W , m ² /g	s_S	d_s , ^(a) Micron	Fuzziness Ratio ^(b)
Lot No.	Calcining Temp., °C				
C-15	As-rec'd.	19.348	0.026	0.159	59.62
C-15	1470	9.870	0.058	0.290	29.85
C-15	1840	5.832	0.113	0.497	16.20
C-15	2170	4.784	---	0.604	11.08
G-26	2500	4.43	0.31	0.650	13.93

(a) Calculated diameter of monosized spheres having specific surface area measured

(b) Ratio of specific surface area measured by BET to that calculated from Micromerograph sample statistics
(Table V)

iation (CV_d). Both measured (BET) surface area, Table VI, and "fuzziness ratio" continued to decrease with heat-treatment to higher temperatures, although at a diminishing rate. These differences in particle characteristics among various heat-treated samples from the same grinding batch are unexpectedly large, and are not fully understood.

The graphites of Series 66 and 73 were all made by solvent-blending with Barrett 30MH coal-tar pitch, hot-molding using "Program A," and graphitizing in argon to temperatures between 2700 and 2800°C. In all cases except those of Specimens 66F-1 and 66G-1, at least a

slight excess of binder was present. Properties of the graphites of both series are listed in Table VII, and with-grain properties are compared in Fig. 3. There are a few points which scatter quite broadly, but in general the trends of the data are clear and the differences between the two series of graphites are relatively small.

For both series of graphites, packed filler densities were quite high and increased with filler heat-treatment temperature. This measurement is made in the baked (not-molded) condition, and all but one of the fillers -- for which the measurement could not be made -- had previously been heat-treated to some temperature higher

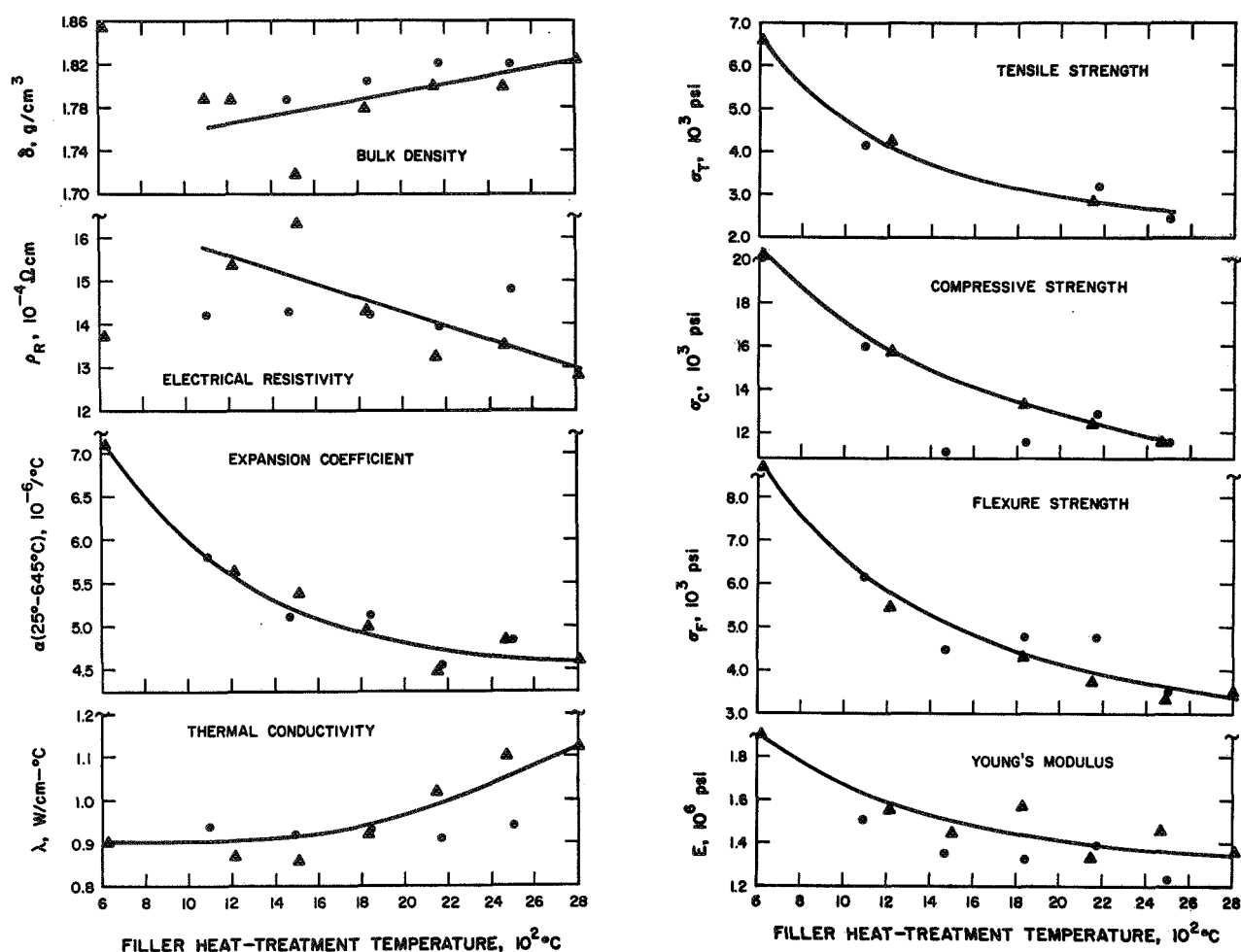


Fig. 3. With-grain properties of Series 66 graphites (triangles) and of Series 73 graphites (circles) as functions of the temperature to which the filler was heat-treated.

than the baking temperature of 900°C . In the case of the Series 66 graphites, the density variation was attributed to a systematic change in filler-particle size distribution. It is not clear that this is true for the Series 73 graphites, the fillers for which were more nearly alike and did not vary monotonically in their distribution parameters. Here there appears to have been a direct effect of filler heat-treatment temperature on packing density. Bulk density in the baked condition increased with packed filler density. As would be expected, shrinkage during graphitizing was greater for fillers calcined at lower

temperatures. However, except for Specimen 66E-1, which was exceptional in several ways, this decrease in bulk volume was not sufficient to compensate for the better packing of fillers calcined to higher temperatures. The trend of bulk density in the graphitized condition was therefore to increase with filler heat-treatment temperature, at least for temperatures above about 1400°C .

It is not clear to what degree the other properties of these graphites, plotted in Fig. 3, are affected simply by this variation in bulk density. The trends of the electrical resistivity and thermal conductivity curves might be

TABLE VII

PROPERTIES OF MOLDED SANTA MARIA GRAPHITES, SERIES 66 AND 73

SPECIMEN NO.:	FILLERS HEAT-TREATED BEFORE GRINDING							FILLERS HT.-TR'T'D. AFTER GRINDING				
	66E-1	66F-1	66G-1	66H-1	66 I-1	66J-1	66K-1	73C-1	73D-1	73E-2	73F-1	73G-2
Calcining Temp., °C	620	1215	1515	1833	2147	2468	2808	1090	1470	1840	2170	2500
Density, g/cm ³	1.853	1.788	1.718	1.779	1.799	1.795	1.824	1.788	1.787	1.805	1.821	1.820
Tensile Str., psi												
With-grain	6656	4224	---	---	2838	---	---	4106	---	---	3171	2430
Compr. Str., psi												
With-grain	20,213	15,867	---	13,278	12,439	11,490	---	15,097	11,027	11,533	12,811	11,476
Across-grain	20,593	15,704	13,031	13,876	12,321	11,965	11,824	15,193	12,649	13,547	13,105	12,275
Flexure Str., psi												
With-grain	8744	5456	---	4280	3715	3355	3496	6129	4478	4780	4739	3493
Across-grain	6468	5833	4620	4826	4084	3846	3421	6391	3822	4702	3966	3058
CTE, x 10 ⁻⁶ /°C ^(a)												
With-grain	7.09	5.64	5.37	4.98	4.47	4.84	4.61	5.80	5.11	5.13	4.54	4.84
Across-grain	7.85	6.58	6.43	5.14	5.73	5.45	5.04	5.97	5.67	5.29	5.59	5.73
Resistivity, μΩcm												
With-grain	1371	1533	1632	1427	1323	1350	1279	1418	1429	1425	1394	1480
Across-grain	1609	1688	1834	1598	1443	1507	1458	1564	1567	1559	1542	1647
Therm. Cond., W/cm-°C												
With-grain	0.90	0.87	0.86	0.92	1.02	1.10	1.12	0.94	0.92	0.93	0.91	0.94
Across-grain	0.77	0.74	0.74	0.86	0.93	1.01	1.02	0.90	0.86	0.88	0.86	0.79
Young's Mod., 10 ⁶ psi												
With-grain	1.897	1.550	1.458	1.569	1.327	1.452	1.363	1.453	1.341	1.332	1.387	1.226
Across-grain	1.621	1.395	1.300	1.406	1.408	1.306	1.291	1.398	1.160	1.178	1.225	1.038
Anisotropies												
BAF ^(b)	1.082	1.065	1.075	1.037	1.034	1.049	1.076	1.049	1.036	1.045	1.050	1.049
Compr. Str.	1.02	0.99	---	1.05	0.99	1.04	---	1.01	1.15	1.18	1.02	1.07
Flexural Str.	1.35	0.94	---	0.89	0.91	0.87	1.02	0.96	1.17	1.02	1.19	1.14
CTE	1.11	1.17	1.20	1.03	1.28	1.13	1.09	1.03	1.11	1.03	1.23	1.18
Resistivity	1.17	1.10	1.12	1.12	1.09	1.12	1.14	1.10	1.10	1.09	1.11	1.11
Therm. Cond.	1.17	1.18	1.16	1.07	1.10	1.09	1.10	1.04	1.07	1.06	1.06	1.19
Young's Mod.	1.17	1.11	1.12	1.12	0.94	1.11	1.06	1.04	1.16	1.13	1.13	1.18

(a) Coefficient of thermal expansion, Average, 25-645°C

(b) Bacon Anisotropy Factor, σ_{02}/σ_{0x}

explained entirely on that basis. However, a density increase would be expected to increase the strength properties, elastic modulus, and thermal expansion coefficient, and these curves show the opposite trends. There appear to be strong effects of increasing filler heat-treatment temperature in decreasing the tensile, compressive, and flexural strength, the Young's modulus, and the thermal expansion coefficient of a molded, pitch-bonded graphite made from this filler.

The crystalline anisotropies of all graphites in both series are quite low, with no Bacon Anisotropy Factor higher than about 1.08. Anisotropies of other properties

are in most cases somewhat higher than has been common for molded Santa Maria graphites, suggesting some degree of preferred orientation in their defect structures.

The very high strength properties and thermal expansion coefficient of Specimen 66E-1, made from a filler calcined only to 620°C, are of particular interest. Unfortunately, this specimen developed circumferential cracks during hot-molding, presumably because of excessive shrinkage of the filler. Aside from the macrocracks, its microstructure was excellent. It appeared dense and sound with a very fine, random structure. Most of the pores were under 5 μ dia, with a few ranging up to about

15 μ .

All other members of Series 66 showed some optical anisotropy and preferred orientation among the fine filler particles. Spongy networks of fines and binder residue were present between some of the larger filler particles, probably resulting from deficiencies in fines in the 10-30 μ size range. Occasional microcracks up to 900 μ long appeared to have propagated between such spongy areas. The Series 73 graphites had microstructures similar to these but without optical anisotropy, preferred orientation, or significant microcracking.

G. Extruded Graphites

One extruded graphite made from a Santa Maria filler is discussed below in connection with an investigation of an experimental resin binder, EMW 1400.

III. ATHABASCA COKE

A. General

A sample of "Athabasca coke" has been obtained from Great Canadian Oil Sands Ltd. (GCOS), a subsidiary of Sun Oil Co. Ltd., of Fort McMurray, Alberta, Canada. Its detailed characterization is discussed below. It appears to be very similar in structure and behavior to the Santa Maria coke, which has been investigated intensively by CMF-13, and therefore to be another potential filler material for the manufacture of isotropic, high-expansion graphites.

B. Source and Treatment

Athabasca coke is a byproduct of the first commercial exploitation of the vast tar-sand deposits of northern Alberta. GCOS uses bucket-wheel excavators to mine about 100,000 tons of tar sand per day. The bitumen is separated from the sand in a hot-water flotation operation, the froth from which is cleaned by thinning it with naphtha and centrifuging. About 10,000 tons per day of cleaned bitumen, mixed with an approximately equal amount of naphtha, is recovered from the centrifuges. This mixture is preheated in conventional heat exchangers where, at temperatures in the range 260-315°C, the naphtha is flashed off, to be recovered and recycled. The

concentrated bitumen is heated rapidly in tube furnaces to about 480°C, then fed to coke drums 26 ft dia and 65 ft high. The coker distillate is withdrawn at about 450°C and 20-30 psig. It is desulfurized with hydrogen, and a sweet synthetic crude is produced at the rate of about 45,000 bbl per day. This is shipped by pipeline to various Sun Oil Co. refineries. About 2600 tons of delayed coke are also produced per day, part of which is used as fuel for the GCOS steam generators.

Analyses of the coke sample received by CMF-13 from GCOS were made by LASL Group CMB-1. It contained:

H ₂ O =	0.33%	Al =	500 ppm
Ash =	2.71%	K =	500 ppm
Fe =	0.26%	V =	500 ppm
S =	4.84%	Ni =	300 ppm
Si =	0.3%	Ca =	300 ppm
		Na =	200 ppm
		Ti =	200 ppm
		Mg =	150 ppm
		Mn =	100 ppm
		Nb =	100 ppm
		Mo =	100 ppm
		B =	10 ppm

The ash and impurity contents of the coke are high, which would be expected to result from incomplete separation of the bitumen from the associated sand and clay in the hot-water flotation and subsequent centrifuging operations. However, there are similarities with the analysis of Santa Maria coke, particularly in the high sulfur, vanadium, and nickel contents of both. There are also similarities between the Athabasca bitumen and the Santa Maria crude petroleum, notably in their high viscosities and their high contents of sulfur, vanadium, and porphyrins.

C. Microstructure (R. D. Reiswig)

As is illustrated by Fig. 4, the microstructure of the Athabasca coke is essentially the same as that of the Santa Maria coke. It contains radial arrangements of lamellae which, in section, appear as rosettes, between which are areas of fine, randomly oriented, nearly equiaxed, optical domains. The frequency of occurrence of the rosettes appears to be somewhat lower in the Atha-

TABLE VIII
CRYSTALLINE PARAMETERS AND HELIUM DENSITIES OF
HEAT-TREATED ATHABASCA AND SANTA MARIA COKES

Ht. -Trt. Temp., °C	Athabasca Coke			Santa Maria Coke		
	L_c , Å	d_{002} , Å	$\delta_{He}^{(a)}$ g/cm ³	L_c , Å	d_{002} , Å	δ_{He} g/cm ³
As-rec'd ^(b)	22.7	3.45	1.399	21.7	3.45	---
600	17.6	3.44	1.522	---	---	---
620	---	---	---	16.2	3.44	1.599
900	---	---	---	17.7	3.44	1.952
1060	22.7	3.44	1.909	---	---	---
1215	---	---	---	25.1	3.44	1.987
1500	56.8	3.43	2.066	---	---	---
1515	---	---	---	48.0	3.42	2.068
1740	76.9	3.43	---	---	---	---
1833	---	---	---	92.4	3.42	2.106
1925	168	3.419	2.078	---	---	---
2147	---	---	---	196	3.391	2.100
2165	207	3.411	---	---	---	---
2415	308	3.373	2.117	---	---	---
2468	---	---	---	306	3.371	2.137
2775	327	3.370	2.138	---	---	---
2808	---	---	---	390	3.365	2.170
2926	---	---	---	380	3.364	---
3110	---	---	---	415	3.364	---

(a) Particle density, by helium pycnometry

(b) Green condition

basca coke than in the Santa Maria coke, which may be advantageous in reducing the proportion of flaky or acicular fine particles produced when the coke is ground.

D. Effects of Heat-Treatment (R. J. Imprescia, J. A. O'Rourke, H. D. Lewis)

Samples of the Athabasca coke were heat-treated in a carbonaceous atmosphere at temperatures up to 2775°C and examined by x-ray diffraction and helium pycnometry. Mean crystallite thickness, L_c , interlayer spacing, d_{002} , and helium density, δ_{He} , of the heat-treated samples are listed in Table VIII and plotted in Fig. 5 as functions of heat-treating temperature, together with similar data

for heat-treated Santa Maria coke. The responses to heat-treatment of the two materials are very similar. The two curves of helium density vs heat-treating temperature cannot be distinguished. Interlayer spacing appears to decrease a little less rapidly in the temperature interval 1500-2000°C in the case of the Athabasca coke, but at and above about 2400°C the same degree of crystalline order is produced in the two materials. Rates of crystallite growth are essentially the same up to at least 2500°C, although at higher temperatures it appears that the crystallite size of the Athabasca coke may level off at about 330 Å while that of the Santa Maria coke continues to increase to above 400 Å. Additional samples heat-

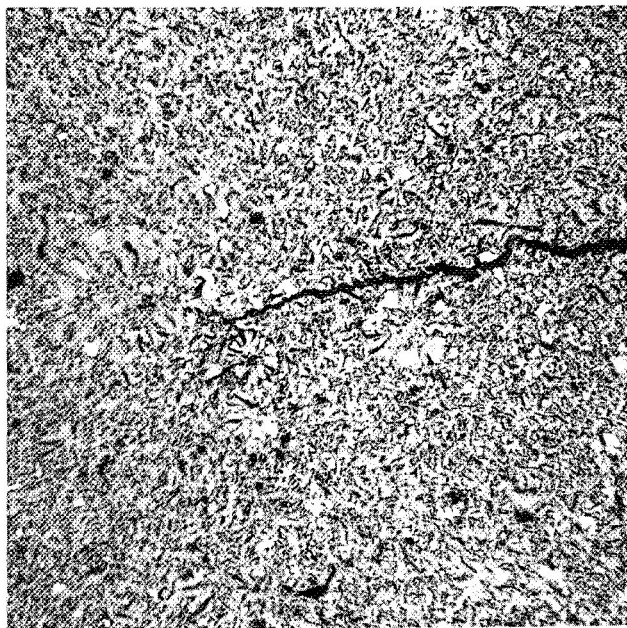


Fig. 4. Typical microstructure of Athabasca coke, showing radial rosette structures similar to those found in Santa Maria coke. Hydrogen-ion etch, 500 X.

treated to above 2500°C will be required to determine whether there is a real difference in the crystallite sizes ultimately attainable in the two cokes. However, both graphitize quite well.

E. Grinding Behavior (R. J. Imprescia, H. D. Lewis)

Filler Lot CP-18 was prepared by calcining a sample of the Athabasca coke and grinding it by Schedule "W + X," which involves two stages of hammer milling. The calcining temperature was intended to be 1100°C, to correspond approximately to the manufacturer's heat-treatment of Santa Maria LV coke. However, because of difficulties in measuring temperature during calcination, the actual temperature was higher than this. From subsequent measurements of crystallite size ($L_c = 35.5 \text{ \AA}$), it is estimated that the actual calcining temperature was 1220°C, which is about 130°C higher than that estimated for Santa Maria LV coke, and which probably reduced the grindability of the Athabasca coke sample.

In Table IX, the characteristics of the ground Athabasca coke (Lot CP-18) are compared with those of Santa Maria LV coke ground in the same way (Lot CP-17).

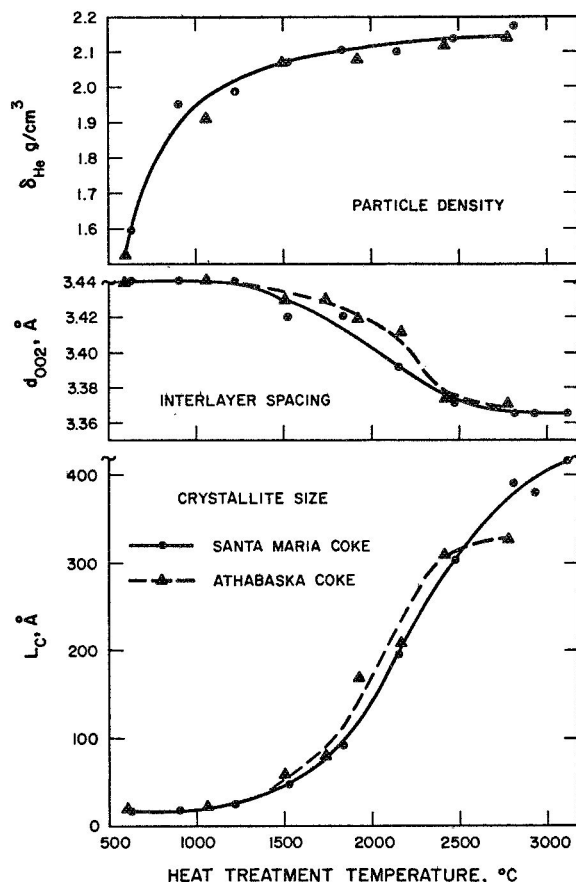


Fig. 5. Effects of heat-treatment on the crystalline parameters and helium density of Athabasca and Santa Maria cokes.

Micromerograph particle-size data for both are plotted in Fig. 6. The Athabasca coke is significantly coarser than the Santa Maria coke, which is probably the result primarily of its higher-temperature calcination. Its distribution curve (Fig. 6) shows the mid-range flattening typical of a Santa Maria coke, which indicates a probable deficiency of particles in the size range about 10 to 40 μ . However, the curve representing the Athabasca coke is more nearly linear than that for the Santa Maria coke, with many more particles at both the fine and the coarse extremes of the curve, indicating a more nearly log-normal distribution of sizes. Therefore, while the grinding behaviors of the two cokes are very similar, the particle-

TABLE IX

PARTICLE CHARACTERISTICS OF SIMILARLY GROUND ATHABASCA AND SANTA MARIA COKES

Sieve Analysis:	Sieve Fraction (U. S. Std. Series)	Weight Percent in Sieve Fraction	
		Athabasca Coke, Lot CP-18 ^(a)	Santa Maria Coke, Lot CP-17 ^(b)
	+ 16	0	0
	-16 + 25	0.5	Tr.
	-25 + 45	17.5	6.8
	-45 + 80	30.5	20.0
	-80 + 170	24.5	31.0
	-170 + 325	10.0	17.2
	- 325	17.0	25.0
Micromerograph Sample Statistics ^(c) :			
	\bar{x}_3	4.853	4.382
	s_x^2	0.165	0.261
	\bar{x}	0.127	0.404
	\bar{d}_3 , microns	269.1	134.8
	\bar{d}_2 , microns	1.292	1.787
	s_d^2 , microns ²	1.486	3.520
	S_W , cm ² /g	950.	1067.
	CV_d	0.944	1.05
Helium Density, δ_{He} , g/cm ³ :		1.96	1.87
BET Surface Area Data:			
	\bar{S}_W , m ² /g	7.651	6.620
	$s_S^{(d)}$	0.08	0.02
	$d_s^{(e)}$, micron	0.399	0.512
Fuzziness Ratio ^(f) :		80.50	58.67

(a) Calcined at approximately 1220°C

(b) Calcined at approximately 1090°C

(c) Finite Interval calculation

(d) Standard deviation of determinations

(e) $d_s = 6/\delta_{He} S_W$

(f) Ratio of measured (BET) surface area to that calculated from Micromerograph data

TABLE X
DENSITIES AND SHRINKAGES OF HOT-MOLDED, PITCH-BONDED GRAPHITES MADE FROM
ATHABASCA AND SANTA MARIA COKES

Specimen No.	Filler Lot No.	Binder Conc., pph	Calculated Optimum Binder, pph	Binder Residue, % (Baked)	Density, g/cm ³			Dimensional Change, Baked to Graph., %		
					Packed Filler (Baked)	Bulk		Δl	Δd	Δv
						Baked	Graph.			
74A-1	CP-18 ^(a)	18	19.4	74.2	1.494	1.694	1.676	-2.0	-2.1	-6.1
74B-1	CP-18	22	18.5	64.2	1.509	1.722	1.700	-1.9	-2.1	-5.9
74C-1	CP-18	26	18.4	56.2	1.511	1.732	1.704	-1.9	-2.1	-6.0
65D-1	CP-17 ^(b)	20	19.0	55.4	1.488	1.653	1.742	-3.8	-3.6	-10.7

(a) Athabasca coke filler

(b) Santa Maria coke filler

size distribution produced may be somewhat more desirable in the case of the Athabasca coke.

In spite of the relative coarseness of the Athabasca coke, its helium density, BET surface area, and fuzziness ratio are all greater than those of the Santa Maria coke. This indicates a higher proportion of surface-connected porosity in the Athabasca coke, which, at least in part, is probably again a result of its higher calcination temperature.

F. Hot-Molded Graphites (R. J. Imprescia)

Three hot-molded graphites have been made from the Athabasca coke flour, Lot CP-18, using Barrett 30MH coal-tar pitch binder, solvent-blending, molding program "A," and graphitization in argon at 2720°C. In Table X, the densities and shrinkages of these graphites are compared with those of a graphite similarly made from the Lot CP-17 Santa Maria flour. The other properties of these graphites are compared in Table XI. These comparisons are probably not fair to the Athabasca filler, since these are the first graphites ever made from it, and Specimen 65D-1 -- with which they are compared -- happens to be one of the best molded graphites of many which have been made from Santa Maria fillers.

When sufficient binder was present, the Athabasca filler packed to a density of about 1.51 g/cm³, which is

relatively high. This was reflected in bulk densities in the baked condition which were significantly higher than that of the Santa Maria graphite, although relatively high binder residues also contributed to this. However, due to greater shrinkage and lower weight loss during graphitizing, the final density of the Santa Maria graphite was significantly higher than the densities of the three Athabasca graphites. The difference in shrinkage is explainable in terms of the lower calcining temperature of the Santa Maria coke. The difference in weight loss is not fully understood, although it is evidently associated with high binder residue in the baked condition.

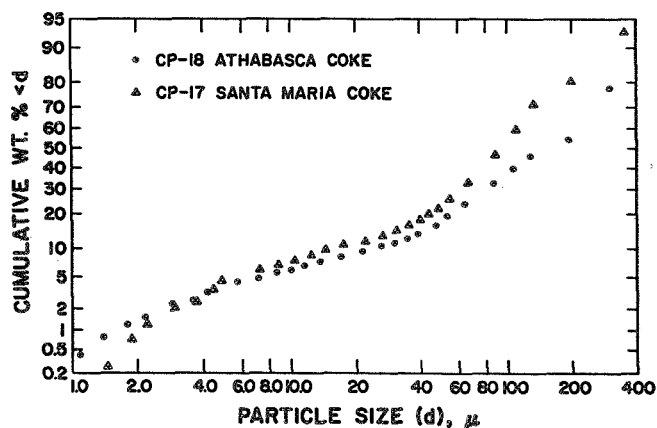


Fig. 6. Micromerograph particle-size data for similarly ground Athabasca coke and Santa Maria coke, calcined at slightly different temperatures.

TABLE XI
PROPERTIES OF GRAPHITES MADE FROM ATHABASCA AND SANTA MARIA COKES

SPECIMEN NO.:	74A-1	74B-1	74C-1	65D-1
Density, g/cm ³	1.676	1.700	1.704	1.742
Tensile Str., psi				
With-grain	1452	1164	1504	3518
Compr., Str., psi				
With-grain	8434	8334	8669	12,015
Across-grain	9588	9258	9995	12,269
Flexure Str., psi				
With-grain	2590	1916	2387	4671
Across-grain	2135	1492	1913	5171
CTE, $\times 10^{-6}/^{\circ}\text{C}$ ^(a)				
With-grain	4.94	5.07	5.34	5.28
Across-grain	5.58	5.98	6.04	5.77
Resistivity, $\mu\Omega\text{cm}$				
With-grain	1757	1724	1719	1250
Across-grain	1604	1792	1686	1263
Therm. Cond., W/cm- $^{\circ}\text{C}$				
With-grain	0.73	0.74	0.74	1.03
Across-grain	0.82	0.74	0.73	0.99
Young's Mod., 10^6 psi				
With-grain	0.765	0.884	0.835	1.21
Across-grain	0.935	0.637	0.652	1.28
Anisotropies:				
BAF ^(b)	1.014	~1.00	1.012	1.022
Comp. Str.	1.14	1.11	1.15	1.02
Flexure Str.	1.21	1.28	1.25	0.90
CTE	1.13	1.18	1.13	1.09
Resistivity	0.91	1.04	0.98	1.01
Therm. Cond.	0.89	1.00	1.01	1.04
Young's Mod.	0.82	1.39	1.28	0.95

(a) Coefficient of thermal expansion, average, 25-645 $^{\circ}\text{C}$

(b) Bacon Anisotropy Factor, σ_{oz}/σ_{ox}

The three Athabasca graphites are reasonably consistent in their properties. All are very nearly isotropic microscopically and crystallographically, although all show some anisotropy in other properties, indicating preferred orientations of their defect structures. Thermal expansion coefficients are high, and approximately equal to that of the Santa Maria graphite. Strength properties are far below those of the Santa Maria graphite, but are creditable for molded graphites of moderate density. Electrical resistivities are high and both thermal conductivities and Young's moduli are low, suggesting that considerable improvements in internal structure of the graphite are possible, which should be reflected in cor-

responding improvements in properties. No gross defects were observed microscopically, but porosities were high and all three Athabasca graphites contained many microcracks -- some up to 400 μ -- adjacent to the larger filler particles. The filler appeared to be deficient in particles finer than about 40 μ . This would contribute both to the poor packing associated with the fine, general porosity, and to the occurrence of relatively thick binder layers whose shrinkage during baking is primarily responsible for microcracking at the filler-binder interfaces. The possibility of improving the microstructure is evident.

In view of the preliminary nature of this work and the complete absence of background information on grinding

TABLE XII
PROPERTIES OF GRAPHITE-ZrC

Specimen Number	Volume Percent ZrC	Bulk Density, g/cm ³	Carbon Residue %	Electrical Resistivity, $\mu\Omega$ cm	Young's Modulus, 10 ⁸ psi
ACP 18	0.16	1.865	44.5	1207	2.34
ACP 17	0.31	1.866	44.2	1212	2.31
ACP 16	0.62	1.876	43.7	1201	2.30
ACP 15	1.24	1.905	43.5	1173	2.33
ACP 6	4.67	2.059	44.0	807	2.61
ACP 7	7.45	2.378	47.0	473	3.47
ACP 8	9.07	2.555	38.9	551	3.07
ACP 9	11.0	2.344	40.5	483	3.28
ACP 10	12.8	2.434	40.3	434	3.52
ACP 11	14.1	2.503	40.9	399	3.63
ACP 12	15.6	2.542	39.4	448	3.45
ACP 13	17.2	2.627	40.4	384	3.77
ACP 14	18.8	2.695	39.3	358	3.97

and packing behavior of the coke, these results are considered to be very encouraging. The Athabasca coke appears indeed to be potentially useful as a filler for the manufacture of isotropic, high-expansion graphites.

IV. GRAPHITE-CARBIDE COMPOSITES

A. Previous Work

The manufacture of a series of extruded graphite-ZrC composites was described in Report No. 14 in this series, pp. 19-21. The mix used consisted of 85 parts G-18 (Great Lakes Grade 1008-S) graphite flour, 15 parts Thermax carbon black, a variable proportion of ZrC powder, and Varcum 8251 furfuryl alcohol resin binder containing 4% maleic anhydride curing catalyst. The mix was extruded as 0.5-in. dia rods which were cured, baked, and graphitized to 2700°C in normal cycles.

B. Properties of Graphite-ZrC Composites (J. M. Dickinson, P. Wagner, D. T. Eash)

Properties of the extruded graphite-ZrC composites are listed in Table XII. As would be expected, bulk density increased linearly with ZrC content (Fig. 7) except for two samples, one of which was made with a large ex-

cess of binder and the other with a deficiency of binder. Binder carbon residue (Fig. 8) scattered more broadly, as is usually the case, with the greatest departures from a linear relation occurring in the two samples which were also abnormal in density. Young's modulus (Fig. 9) is a

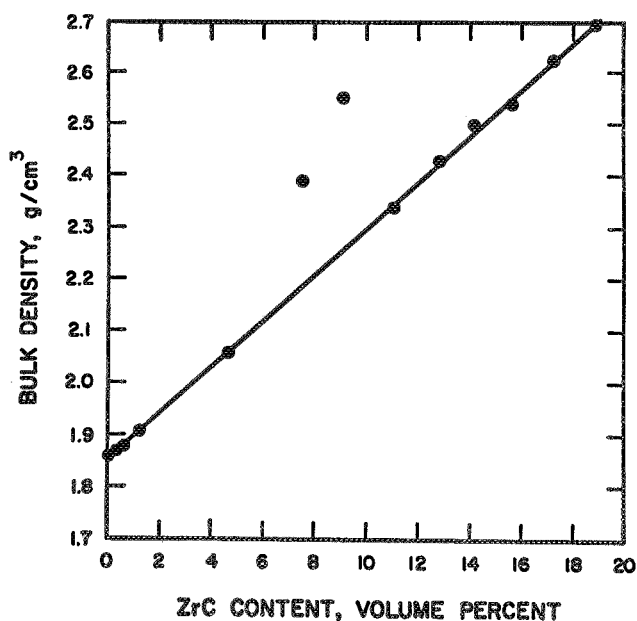


Fig. 7. Effect of ZrC content on bulk density of graphite-ZrC composites.

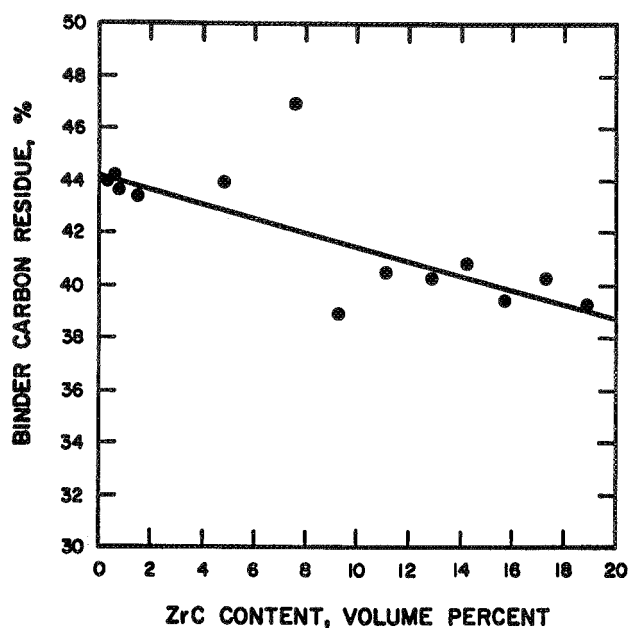


Fig. 8. Relation between ZrC content and binder-carbon residue in graphite-ZrC composites.

smooth function of ZrC content, although it is not clear that the relation is a linear one. In Fig. 10, electrical resistivity has been plotted as a function of mole percent ZrC, and it is evident that the data are affected by manufacturing as well as compositional variables. However,

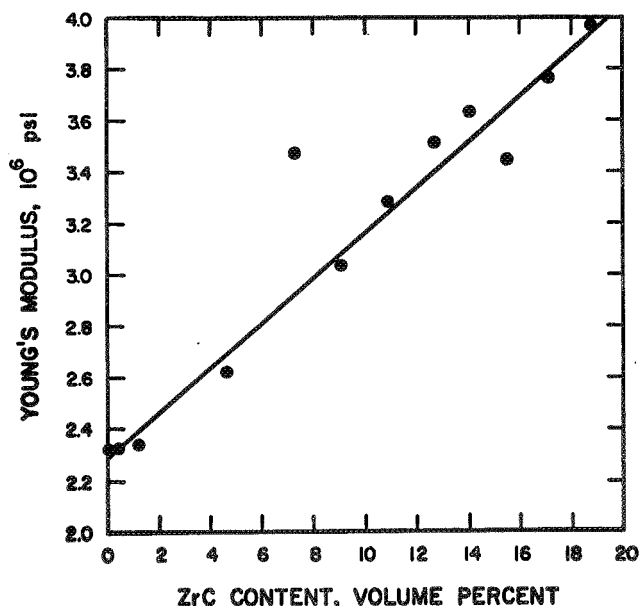


Fig. 9. Effect of ZrC content on Young's modulus of graphite-ZrC composites.

it appears that with careful control of manufacturing procedures, and if necessary by discarding samples which depart widely from properties vs composition curves such as these, it should be possible to produce a series of particulate composites suitable for the planned investigation of the relation between thermal diffusivity and thermal conductivity at high temperatures.

Specimen ACP14, which has the highest ZrC content (18.8 vol %) in this series, has also been tested in compression, flexure, and thermal shock. Compression tests by D. T. Each, CMF-13, gave ultimate strength values of 14,475 and 14,275 psi, for an average compressive strength of 14,375 psi. Flexure tests gave strength values of 7000 psi for a 0.25-in. by 0.375-in. rectangular bar and of 8975 psi for a machined tube 0.25-in. outside diameter with a 0.1-in. dia axial hole. Thermal-shock tests made by C. R. King, N-7, on 0.5-in. dia discs gave a thermal shock index of 157.5/160, which is slightly higher than the indices obtained on similar specimens of SX5 graphite and significantly lower than those obtained on RCV graphite.

Microstructurally, these composites suffered from a uniformity problem. The fine ZrC particles were of course concentrated in the binder residue, and so appeared in discontinuous networks around the coarser filler particles. A more nearly uniform distribution of the carbide would be obtained if a filler were used from which

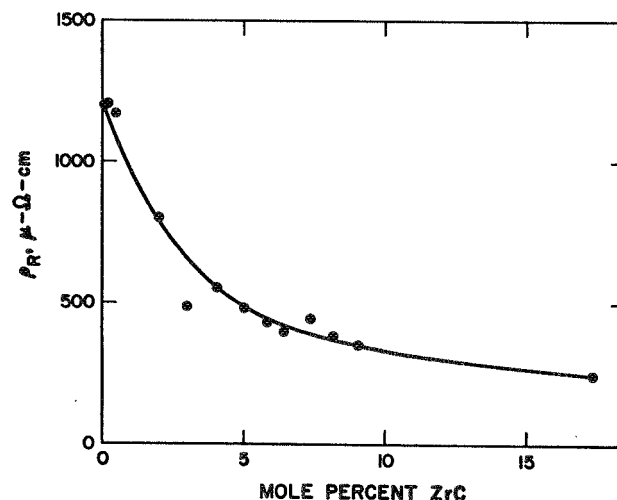


Fig. 10. Effect of ZrC content on electrical resistivity of graphite-ZrC composites.

TABLE XIII
COMPOSITIONS AND EXTRUSION CONDITIONS OF GRAPHITE AND COMPOSITE TUBES

Specimen Number	Extrusion Section	Filler Used	ZrC, Vol %	Binder		Extrusion Conditions			Temperatures	
				Amount	Type	Pressure, psi	Velocity, in./min	Vacuum, Torr	Mix °C	Chamber °C
ACV 1	1	G-18	0	27 pph	Varc. 8251	8100	171	<1000	41	46
ACV 1	2	G-18	0	27 pph	Varc. 8251	9000	200	<1000	41	46
ACV 1	3	G-18	0	27 pph	Varc. 8251	135000	200	600	41	46
ACV 1	4	G-18	0	27 pph	Varc. 8251	7425	97	600	41	46
ACV 2	1	G-26	0	25 pph	Varc. 8251	10125	164	450	41	50
ACV 2	2	G-26	0	25 pph	Varc. 8251	14130	450	450	41	50
ACV 2	3	G-26	0	25 pph	Varc. 8251	15975	800	450	41	50
ACV 2	4	G-26	0	25 pph	Varc. 8251	11430	---	450	41	50
ACV 3	1	G-26	0	25 pph	EMW 1400	20000	257	500	45	50
ACV 3	2	G-26	0	25 pph	EMW 1400	22050	257	500	45	50
ACV4	3	G-26	0	25 pph	EMW 1400	22050	257	500	45	50
ACW 1	1	G-26	30	13.9pph	EMW 1400	19260	200	600	45	49
ACW 1	2	G-26	30	13.9pph	EMW 1400	18630	171	600	45	49
ACW 1	3	G-26	30	13.9pph	EMW 1400	19260	189	600	45	49
ACW 1	4	G-26	30	13.9pph	EMW 1400	21960	288	600	45	49
ACW 1	5	G-26	30	13.9pph	EMW 1400	14400	48	600	45	49
ACW 2	1	G-26	30	13.9pph	Varc. 8251	10080	300	600	45	50
ACW 2	2	G-26	30	13.9pph	Varc. 8251	9450	150	600	45	50
ACW 2	3	G-26	30	13.9pph	Varc. 8251	9900	240	600	45	50
ACW 2	4	G-26	30	13.9pph	Varc. 8251	12151	900	600	45	50
ACW 2	5	G-26	30	13.9pph	Varc. 8251	8251	57	600	45	50

the coarse particles had been removed.

In all cases, moderately thick layers of "reorganized graphite" partially surrounded the carbide particles in the graphitized samples. This is a blocky, highly ordered graphite, resembling a good pyrolytic graphite, which is frequently formed in polycrystalline graphites in the vicinities of heavy-metal inclusions. The mechanism of its formation is not fully understood.

C. Extruded Graphite and Composite Tubes (J. M. Dickinson)

Two series of thin-walled tubes, nominally 0.25-in. outside diameter and 0.10-in. inside diameter, have been

manufactured by extrusion. Series ACV tubes are resin-bonded graphites, made from a mix containing: 85 parts of graphite flour, either CMF-13 Lot G-18 (a Great Lakes grade 1008-S flour) or CMF-13 Lot G-26 (Santa Maria flour, Y-12 "Blend 1"); 15 parts of Thermax carbon black; and either 25 or 27 pph of either Varcum 8251 or EMW 1400 furfuryl alcohol resin, catalyzed with 4% maleic anhydride. Series ACW tubes are graphite-ZrC composites nominally containing 30 vol % of ZrC, made by adding ZrC to the above graphite mix together with additional binder in the proportion 0.077 gram of binder per gram of ZrC.

The dry ingredients of these mixes were blended in

TABLE XIV
PROPERTIES OF GRAPHITE AND COMPOSITE TUBES

Specimen No.	ZrC vol %	Binder	Heat Treatment	Bulk Density, g/cm ³	Carbon Residue, %	Resistivity, $\mu \Omega \text{ cm}$	Young's Modulus, 10 ⁶ psi	CTE, ^(a) $\times 10^{-6}/^{\circ}\text{C}$
ACV1-1	0	Varc. 8251	Normal	1.803	36.6	1309	2.09	2.17
ACV1-2	0	Varc. 8251	Normal	1.810	37.4	1301	2.11	---
ACV1-3	0	Varc. 8251	Normal	1.827	38.2	1278	2.17	---
<u>ACV1-4</u>	<u>0</u>	<u>Varc. 8251</u>	<u>Normal</u>	<u>1.789</u>	<u>36.9</u>	<u>1333</u>	<u>2.06</u>	<u>---</u>
Average	0	Varc. 8251	Normal	1.807	37.3	1303	2.11	2.17
ACV2-1	0	Varc. 8251	Normal	1.792	37.7	1934	1.35	4.61
ACV2-2	0	Varc. 8251	Normal	1.768	38.0	1979	1.31	---
ACV2-3	0	Varc. 8251	Normal	1.788	36.9	1972	1.37	---
<u>ACV2-4</u>	<u>0</u>	<u>Varc. 8251</u>	<u>Normal</u>	<u>1.780</u>	<u>36.1</u>	<u>2042</u>	<u>1.29</u>	<u>---</u>
Average	0	Varc. 8251	Normal	1.782	37.2	1982	1.33	4.61
ACV3-1	0	EMW 1400	Normal	1.839	---	1817	1.56	---
ACV3-2	0	EMW 1400	Normal	1.823	---	1904	1.50	4.75
<u>ACV3-3</u>	<u>0</u>	<u>EMW 1400</u>	<u>Normal</u>	<u>1.820</u>	<u>---</u>	<u>1904</u>	<u>1.49</u>	<u>---</u>
Average	0	EMW 1400	Normal	1.827	---	1875	1.52	4.75
ACV3-1	0	EMW 1400	Slow	---	---	1832	1.55	---
ACV3-2	0	EMW 1400	Slow	1.832	---	1911	1.48	---
<u>ACV3-3</u>	<u>0</u>	<u>EMW 1400</u>	<u>Slow</u>	<u>---</u>	<u>---</u>	<u>1911</u>	<u>1.47</u>	<u>---</u>
Average	0	EMW 1400	Slow	1.832	---	1888	1.50	---
ACW1-1	30	EMW 1400	Slow	3.151	38.3	233	5.33	---
ACW1-2	30	EMW 1400	Slow	3.159	37.9	223	5.43	---
ACW1-3	30	EMW 1400	Slow	3.160	36.5	231	5.34	---
ACW1-4	30	EMW 1400	Slow	---	36.1	230	5.40	---
<u>ACW1-5</u>	<u>30</u>	<u>EMW 1400</u>	<u>Slow</u>	<u>3.168</u>	<u>36.8</u>	<u>233</u>	<u>5.42</u>	<u>---</u>
Average	30	EMW 1400	Slow	3.160	37.1	229	5.38	---
ACW1-1	30	EMW 1400	Normal	---	37.7	241	4.98	6.51
ACW1-2	30	EMW 1400	Normal	3.107	37.7	227	5.17	---
ACW1-3	30	EMW 1400	Normal	3.146	36.5	234	5.06	---
ACW1-4	30	EMW 1400	Normal	3.149	36.7	232	5.04	---
<u>ACW1-5</u>	<u>30</u>	<u>EMW 1400</u>	<u>Normal</u>	<u>3.127</u>	<u>35.6</u>	<u>231</u>	<u>5.17</u>	<u>---</u>
Average	30	EMW 1400	Normal	3.132	36.8	232	5.10	6.51
ACW2-1	30	Varc. 8251	Normal	3.057	33.2	234	4.87	---
ACW2-2	30	Varc. 8251	Normal	3.075	32.8	231	4.83	5.50
ACW2-3	30	Varc. 8251	Normal	3.091	33.2	224	4.88	---
ACW2-4	30	Varc. 8251	Normal	3.072	33.5	245	4.80	---
<u>ACW2-5</u>	<u>30</u>	<u>Varc. 8251</u>	<u>Normal</u>	<u>3.081</u>	<u>33.8</u>	<u>235</u>	<u>4.82</u>	<u>---</u>
Average	30	Varc. 8251	Normal	3.075	33.3	234	4.84	5.50

(a) Coefficient of thermal expansion, average, 25-645°C. With-grain orientation.

a twin-shell blender. The binder was hand-kneaded into the dry mix, and the wet mix was then blended 15 min in a twin-shell blender using an intensifier bar. Normal multiple extrusion was used, with intermediate chopping in a food-chopper. Because of limitations of the runout arrangement, each final extrusion was made in several 7-ft sections, usually with variations in extrusion pressure from one section to the next, as is indicated in Table XIII. Each section was cut into 8-in. lengths, which were cured, baked, and graphitized in normal cycles. The graphite tubes were graphitized to 2800°C and the composite tubes only to 2700°C, to avoid the possibility of eutectic melting.

Properties of these materials are listed in Table XIV. Densities were measured by LASL Group CMB-1, using paraffin-coated specimens and an immersion technique.

Compared with similar graphites previously extruded as 0.5-in. dia bars, the graphites of the ACV series had relatively low densities, carbon yields, and Young's moduli, and high electrical resistivities. These deficiencies may result in part from the geometry of a thin-walled tube, which has a much higher surface-to-volume ratio than do the rods usually made. However, properties can probably be increased by improved design of the die-set, which is being undertaken. In the meantime, like the graphites, the composites of the ACW series can undoubtedly be improved by improving the die design.

The ACV graphites extruded at higher pressures in general had slightly better properties, even though the pressure increase was accompanied by an increase in extrusion rate. (ACV-3 was exceptional in this regard, because of an apparent "drying out" of the mix in the press.) Higher properties were obtained with the G-18 filler than with G-26 flour, with a much lower thermal expansion coefficient and undoubtedly a much greater anisotropy. The use of the higher-viscosity EMW 1400 resin (viscosity about 1400 cp) produced significant improvements. Use of a very slow curing cycle, which is important when thick sections are made with a high-viscosity resin, had little apparent effect on these thin-walled tubes.

For the ACW composites, EMW 1400 was also the better binder. However, in this case extrusion pressure

and speed did not appear to be important variables. Use of the slow curing cycle with the high-viscosity binder was an advantage with the composites.

The microstructures of the composites were very "tight" compared to those of the graphite tubes. In the case of the G-26 Santa Maria filler, the ZrC particles were in the right size range to correct a deficiency in the particle-size distribution of the graphite flour, so that particle packing was actually better in the composites than in the corresponding graphites. Further, a considerable proportion of reorganized graphite formed around the ZrC particles during graphitization, and where this reorganization occurs the characteristic defects of a polycrystalline graphite seem to disappear. The microstructures of the composites made from the Santa Maria flour with the high-viscosity binder were exceptionally good. These composites also had the highest expansion coefficients found in this series.

V. FURFURYL ALCOHOL BINDER RESINS

A. Quaker Oats Co. Experimental Resins (E. M. Wewerka)

Two samples of relatively high viscosity furfuryl alcohol resins have been received from the Quaker Oats Co. for investigation as possible binder materials for graphite manufacture. Both are experimental resins, identified by Quaker Oats as QX247 (viscosity 880 cp) and QX248 (2000 cp). Gel-permeation chromatography has been used to compare them with resins of similar viscosities prepared by CMF-13. The chromatograms were analyzed by the method described in Report No. 8 of this series, in which the chart is arbitrarily subdivided into four sequentially numbered regions representing fractions having progressively larger mean molecular sizes. Results of this analysis are listed in Table XV.

At comparable viscosities, the Quaker Oats resins have considerably larger proportions both of monomer-size molecules (Fraction No. 1) and of high molecular-weight species (Fraction No. 4) than do the CMF-13 resins. On the basis of previous CMF-13 experience, molecular-size distributions peaking more sharply in the intermediate-size region would be preferred in a binder resin. However, the Quaker Oats resins represent a

TABLE XV
PROPORTION OF RESIN IN EACH SIZE FRACTION OF THE GPC CURVE

Identification	Resin Viscosity, cp	Fraction No.			
		1	2	3	4
EMW 304	2050	9.0%	37.4%	42.1%	11.5%
QX 248	2000	12.5%	34.3%	37.4%	15.9%
EMW 305	960	10.8%	39.3%	38.9%	11.1%
QX 247	880	15.2%	33.9%	35.5%	15.4%
EMW 1400	1400	11.3%	37.7%	39.4%	11.6%

substantial improvement in this respect over the Varcum 8251 resin that has normally been used here.

B. Lactone Component of Alumina-Polymerized Resins
(E. M. Wewerka)

As has previously been reported, the carbonyl component of γ -alumina polymerized furfuryl alcohol resins prepared in CMF-13 has been firmly identified as 4-methyl, 4-furfuryl, 2-en- γ -butyrolactone (" γ -BL"). The early reports on such resins by Armour Research Foundation did not indicate the presence of γ -BL, but did identify "esters of levulinic acid" as resin components (C. W. Boquist et al, WADD Technical Report 61-72, Vol. XV, 1963). These have not been found in the CMF-13 resins.

The Armour resins were prepared by the methods detailed in Nielsen's patent (U. S. Patent 2, 681, 896 issued 1954). The CMF-13 procedures are generally similar to these, but differ from them in some details. In particular, in the CMF-13 process the γ -alumina catalyst is heated together with furfuryl alcohol in a reaction flask equipped with a Vigreux-type condenser, and the water and some of the furfuryl alcohol are allowed to escape from the top of the condenser during the reaction. Nielsen, however, trapped all of the volatile materials, removed the water from them, and returned the rest to the reaction flask.

To determine whether this difference in procedure resulted in a difference in resin components, a 300 cp resin was made using the Nielsen method. Volatile materials were recovered in a water-cooled condenser and

allowed to drip into a Dean-Stark trap, from which the heavier, nonaqueous layer was continuously returned to the reaction flask. The resin produced was fractionated by distillation, and its individual low-molecular-weight components were separated by gas chromatography and identified. Results are listed in Table XVI. Significant amounts of γ -BL were present, and no levulinic acid esters could be detected. Apparently the identification of the latter by the Armour group represented an incorrect assignment of structure to what was actually the γ -butyrolactone.

This resin, produced precisely as described in the Nielsen patent, did not differ in any major respect from

TABLE XVI
DISTRIBUTION OF LOW-MOLECULAR-WEIGHT
COMPONENTS IN A 300 CP FURFURYL ALCOHOL RESIN
PRODUCED BY NIELSEN'S METHOD OF
CATALYSIS WITH γ -ALUMINA

Component	% of Low M.W. Fraction	% of Total Resin
Furfuryl Alcohol	24	8
Difurylmethane	11	4
Difurfuryl Ether	36	12
γ -BL	18	6
2,5-Difurfuryl Furan	11	4
H ₂ O	Tr	Tr
Total Accounted for:	100%	34%

TABLE XVII
COMPOSITIONS AND EXTRUSION CONDITIONS FOR GRAPHITES MADE WITH EMW 1400 RESIN

Specimen Number	Filler Flour	Binder ^(a) Content, pph	Extrusion Conditions			Temperatures		Green dia., in.
			Pressure, psi	Velocity, in./min	Vacuum, μ	Mix, °C	Chamber, °C	
ACK 4	G-29	27	6075	171	550	52	50	0.5015
ACI 11	G-26	25.5	≈5625	171	600	57	52	0.5005
ACE 8	G-18	27	6075	171	1000	56	51	0.5035

(a) EMW 1400 catalyzed with 4% maleic anhydride

resins of similar viscosity made by normal CMF-13 procedures using γ -alumina as the catalyst.

C. Synthesis of γ -BL (E. M. Wewerka, R. J. Barreras)

Work has continued on the independent synthesis of the γ -butyrolactone found to exist in alumina-polymerized furfuryl alcohol resins, using a synthetic scheme outlined in Report No. 14 in this series.

Some difficulty was experienced in producing furfuryl methyl ketone (product No. 4 in the reaction sequence) from the nitroolefin by the use of iron in hydrochloric acid. The reaction was therefore carried out by treating the nitroolefine with a solution of zinc and hydrochloric acid. There was some delay in identifying the reaction product as furfuryl methyl ketone because, as was established by a more lengthy identification process, a published infrared spectrum of this compound is erroneous.

The next step in the proposed synthesis is the reaction of sodium acetylide with furfuryl methyl ketone. Conditions have been established which cause the acetylide to react with other ketones, such as acetone. However, the desired reaction with furfuryl methyl ketone has not been made to occur, perhaps because of enolization by the acetylide. Other methods of acetylating furfuryl methyl ketone are therefore being investigated.

D. Extruded Graphites Made from EMW 1400 Resin

(J. M. Dickinson)

EMW 1400 is a furfuryl alcohol resin having a relatively narrow molecular-size distribution, which was prepared by acid-polymerizing the monomer directly to

a viscosity of 1400 cp. Because its viscosity was slightly lower than that of EMW 1600, it was expected to be somewhat easier to handle in the graphite-manufacturing process.

The three extruded graphites listed in Table XVII were made using EMW 1400 resin catalyzed with 4% maleic anhydride, with the following three graphite flour fillers: CMF-13 Lot G-29, a Great Lakes Grade 1008-S flour; CMF-13 Lot G-26, the Y-12 "Blend 1" Santa Maria flour; and CMF-13 Lot G-18, another lot of the 1008-S flour. In each case, Thermax carbon black was added to the mix in the proportion 15 parts Thermax to 85 parts graphite flour.

Properties of these graphites are listed in Table XVIII, where they are compared with similar graphites previously made with the slightly more viscous (1600 cp) EMW 1600 resin. The differences are not large.

Microstructural examination showed that most of these graphites contained some microcracks 50 to 100 μ long. An axial crack was observed in graphite ACK 4, made from G-29 flour and EMW 1400 resin, and a similar crack was found in graphite ACI 11, made from G-26 flour and EMW 1400 resin. Bulk densities of these graphites were 1.93 and 1.90 g/cm³ respectively, which are high enough so that the appearance of some defects in the extruded rods is difficult to avoid. However, from the work on tubes reported above, it appears that this problem may not appear in extrusions having thinner sections.

In general, behavior of the EMW 1400 resin binder was essentially the same as that of the EMW 1600 binder,

TABLE XVIII
PROPERTIES OF EXTRUDED GRAPHITES MADE WITH EMW 1400 AND EMW 1600 RESINS

Specimen No.	Filler	Binder	Condition	Bulk Density, g/cm ³	Binder Carbon Residue, %	Electrical Resistivity, $\mu \Omega$ cm	Young's Modulus, 10 ⁶ psi
ACK 4	G-29	EMW 1400	Cured	---	87.8	---	---
ACK 4	G-29	EMW 1400	Baked	---	53.5	---	---
ACK 4	G-29	EMW 1400	Graph.	1.929	51.7	1101	2.44
ACK 2	G-29	EMW 1600	Graph.	1.920	51.0	1145	2.30
ACI 11	G-26	EMW 1400	Cured	---	87.5	---	---
ACI 11	G-26	EMW 1400	Baked	---	53.7	---	---
ACI 11	G-26	EMW 1400	Graph.	1.899	51.5	1645	1.73
ACI 7	G-26	EMW 1600	Graph.	1.906	50.2	1368	1.79
ACE 8	G-18	EMW 1400	Cured	---	87.5	---	---
ACE 8	G-18	EMW 1400	Baked	---	51.6	---	---
ACE 8	G-18	EMW 1400	Graph.	1.914	49.8	1100	2.67
ACE 3	G-18	EMW 1600	Graph.	1.908	49.5	1105	2.57

and its lower viscosity is an advantage in the mixing and extrusion operations.

VI. PARTICLE PACKING

A. Graphite-ZrC Composites (H. D. Lewis)

The extruded graphite-ZrC composites discussed above were made from Lot G-26 Santa Maria graphite flour, a furfuryl alcohol resin binder, and an addition of

Lot ZrC-77-D zirconium carbide powder sufficient to produce a particulate composite containing 30 volume percent ZrC. It was observed that the microstructures of the composites represented a distinct improvement over those of graphites made from the same filler without the ZrC addition, suggesting better particle packing in the case of the mixed filler.

Micromerograph particle-size data for the graphite filler and the ZrC powder are plotted in Figs. 11 and 12,

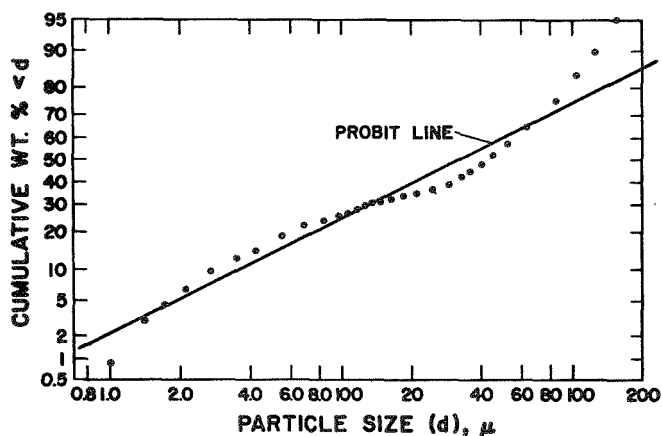


Fig. 11. Log-probability plot of Micromerograph particle-size data for Santa Maria graphite flour, CMF-13 Lot G-26.

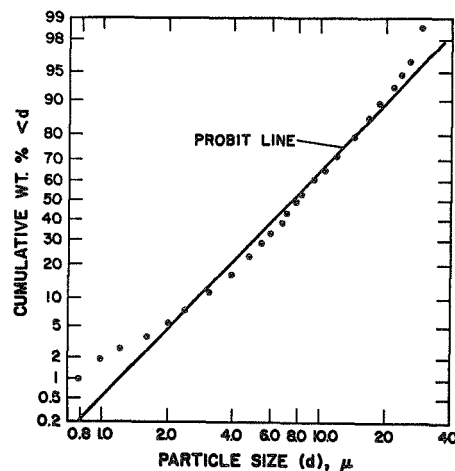


Fig. 12. Log-probability plot of Micromerograph particle-size data for zirconium carbide powder, Lot ZrC-77-D.

TABLE XIX

SAMPLE STATISTICS (INTERVAL MODEL)
FOR SANTA MARIA GRAPHITE FLOUR, LOT G-26,
AND ZIRCONIUM CARBIDE POWDER, LOT ZrC-77-D

	Graphite Flour (G-26)	ZrC Powder (ZrC-77-D)
\bar{x}_3	3.317	2.016
s_x^2	0.177	0.285
\bar{x}	0.218	-0.014
\bar{d}_3 , microns	57.55	9.670
\bar{d} , microns	1.410	1.214
s_d^2 , microns ²	1.050	1.402
S_W , cm ² /g	3181	1703
CV_d	0.730	0.976

and sample statistics derived from these data are compared in Table XIX. As is usually true of Santa Maria fillers, there is a "hole" in the particle-size distribution of the Lot G-26 flour, represented by a flattening of the curve of Fig. 11 between about 10 and about 30 μ . The ZrC powder is much finer and more nearly lognormal than is the graphite filler. These differences are emphasized in Fig. 13, where weight-fraction diagrams of the

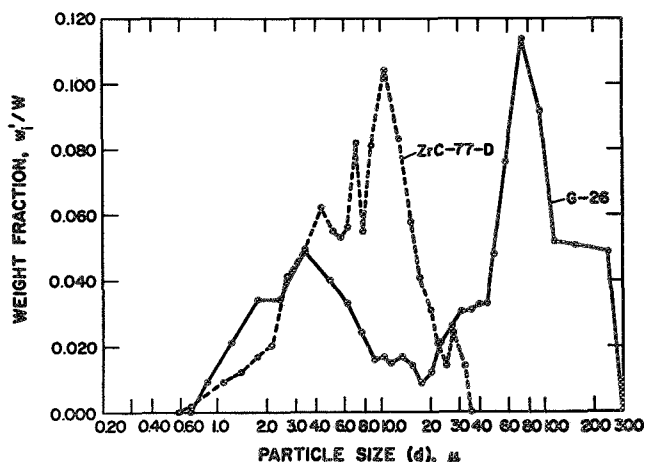


Fig. 13. Weight-fraction diagrams for Lot G-26 graphite flour and Lot ZrC-77-D zirconium carbide powder.

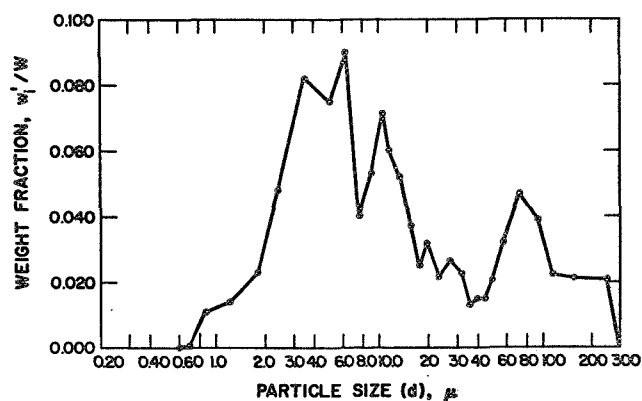


Fig. 14. Weight-fraction diagram for a mixture of 30 volume % ZrC-77-D powder with 70 volume % Lot G-26 graphite flour.

two materials are plotted together. The bimodal character of the G-26 distribution is evident, and it appears that the size range containing the greatest proportion of ZrC particles happens to correspond roughly with the "hole" in the G-26 distribution. As is evident in Fig. 14, a mixture of 30 volume % (57.3 wt %) ZrC with 70 volume % (42.7 wt %) of the graphite flour was less obviously bimodal in character than was the graphite flour alone, and was positively skewed. According to the Lewis-Goldman packing model, both of these changes should increase particle-packing efficiency. However, since these are weight-fraction diagrams and since ZrC and graphite differ widely in density, it is not obvious from the figures how the volume relations which actually control packing have been affected. The weight-fraction diagram of Fig. 14 was therefore transformed to the volume-fraction diagram of Fig. 15. Although the "hole" in the distribution between about 10 and 30 μ still exists, it is less pronounced than for the original G-26 flour (Fig. 13), and the proportion of fine (< 10 μ) particles available to fill voids between large filler particles has been greatly increased.

Since it appeared that a further improvement in packing behavior might be accomplished by adjusting the proportion of ZrC added to the mixture, an attempt was made to optimize mixture composition by using the FININT computer program to analyze the particle-size data for the ZrC and graphite flour. The output listing CV_d (coefficient of variation) vs weight fraction ZrC in the mixture

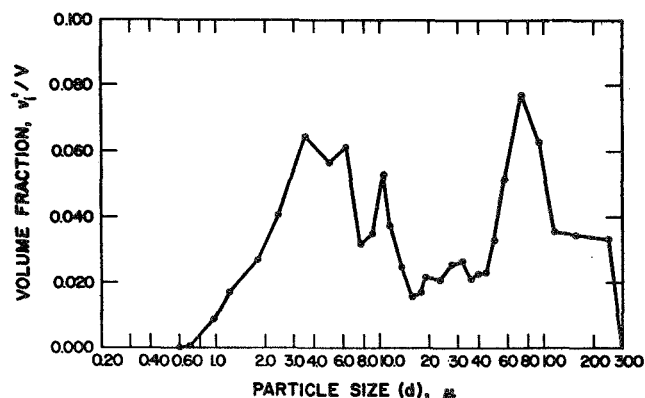


Fig. 15. Volume-fraction diagram for the same mixture represented by Fig. 14.

is shown in Fig. 16. According to the maximum variance-coefficient of variation model, the monotonic increase in CV_d from 0 to 100% ZrC indicates a corresponding monotonic increase in packing efficiency, and there is no optimum ZrC addition which will maximize packing efficiency.

The volume-fraction diagram for the mixture, Fig. 15, does suggest a way in which a positively skewed, uni-modal distribution could be produced in order to further improve packing efficiency. This could be done by screening out about 85 wt % of the material between 40 and 100 μ dia and about 90 wt % of the material coarser than 100 μ dia, which would still leave enough of the coarse particles so that the mixture should behave well in extrusion and heat-treatment.

VII. EFFECTS OF POROSITY ON GRAPHITE PROPERTIES

A. Previous Work

The effects of porosity on the properties of graphites have been discussed in Reports 11-14 in this series.

B. Properties of Santa Maria Graphites (P. E. Armstrong)

During 1969 and 1970, data have been accumulated on a wide variety of experimental graphites made from Santa Maria fillers. These graphites have been made

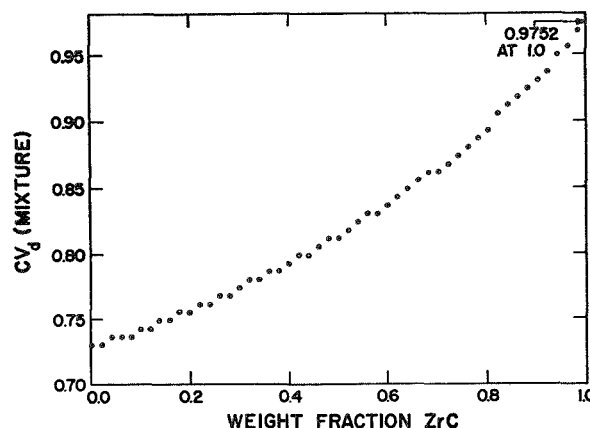


Fig. 16. Effect of increasing weight-fraction of ZrC on the coefficient of variation of the ZrC-graphite flour mixture.

both by molding and by extrusion, under a variety of conditions, using variously heat-treated fillers ground in several different ways. Both resin and pitch binders have been used, and carbon black has sometimes been added to the mix. The graphites produced have ranged from very good to very bad.

Dynamic Young's moduli of these Santa Maria graphites have been plotted as a function of fractional porosity in Fig. 17. As would be expected, the scatter of modulus values is very broad. The line plotted in the figure represents a least-squares fit to the data on POCO graphites previously reported. Except for some of the most dense extruded graphites, this line appears to represent an upper bound on the moduli of Santa Maria graphites.

If it is assumed that a dynamic modulus measurement is not sensitive to the same defects that tend to reduce strength seriously, then a plot of strength vs modulus would be expected to indicate an upper bound on the strength to be expected at a given modulus. Figure 18 is a plot of compressive strength vs Young's modulus for Santa Maria graphites. An arbitrary upper bound on the strength values is indicated by the line, which represents the equation

$$C = -5.4 + 14.7 E,$$

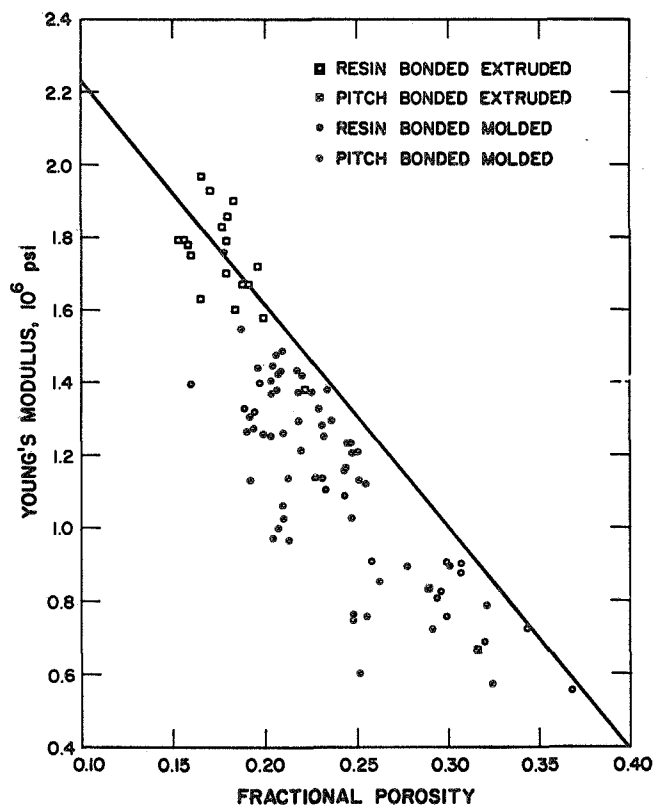


Fig. 17. Young's moduli of Santa Maria graphites as a function of fractional porosity. The line indicates this relation for POCO graphites.

where C is compressive strength in thousands of pounds per square inch and E is dynamic Young's modulus in millions of pounds per square inch. Of particular interest are the relatively low compressive strengths of the extruded resin-bonded graphites. These may result from a preferred arrangement of defects produced by material flow in the extrusion operation.

In Fig. 19 the flexure strengths of molded Santa Maria graphites have been plotted against their dynamic Young's moduli. (Flexure strengths have not been measured on extruded graphites of this type.) Again an arbitrary upper bound on the strength values is indicated by a line, representing the equation

$$F = -2.3 + 6.3 E,$$

where F is flexure strength in thousands of psi and E is dynamic Young's modulus in millions of psi. Except for one measurement, the data appear to group well below

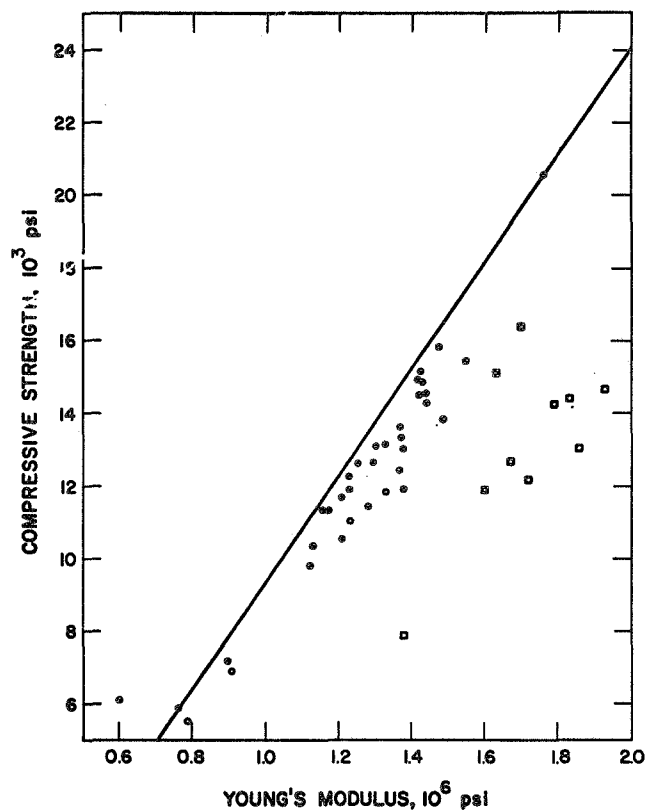


Fig. 18. The relation between compressive strength and dynamic Young's modulus for Santa Maria graphites.

the line.

This type of analysis appears to be useful in at least two ways. First, if lines such as those of Figs. 18 and 19 do represent the upper limits of strength at a given modulus, then a comparison of the strength of a given graphite with the line value at the appropriate modulus indicates how much improvement in strength properties might be accomplished by improving manufacturing procedures. The scatter of modulus values in Fig. 17 suggests that this estimate will necessarily be quite uncertain, but any indication of the probable reward from such a development effort is useful in deciding whether the effort should be made. Second, such plots offer a basis for comparing groups of graphites which differ in some specific way. Thus, the above data indicate that, for molded Santa Maria graphites, the strength-modulus-porosity relation is essentially the same whether a pitch binder or a resin binder is used. This would probably not have been predicted.

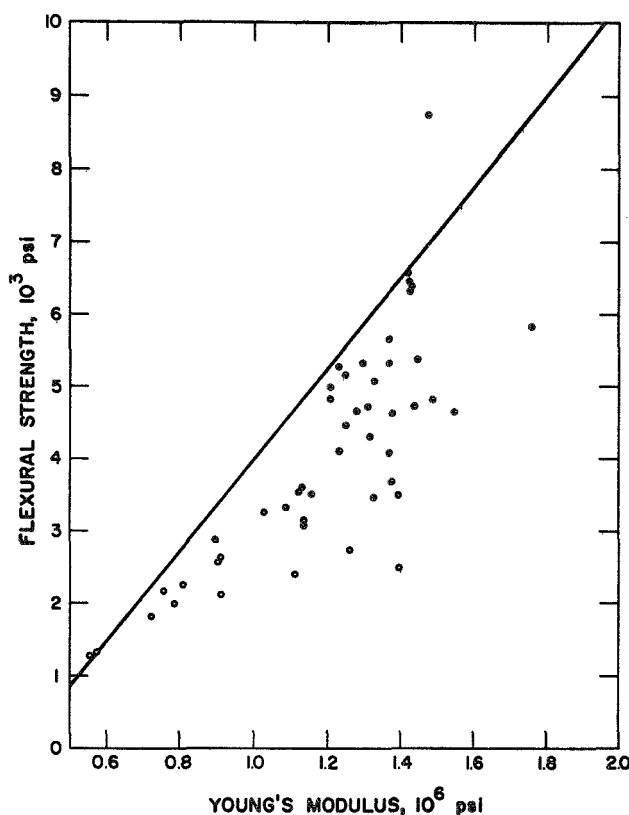


Fig. 19. The relation between flexure strength and Young's modulus for molded Santa Maria graphites.

C. Temperature Dependence of Young's Modulus (P. E. Armstrong)

Experiments have been started to determine the temperature dependence of Young's modulus of a series of POCO graphites which differ significantly only in density. The results will be used to compare the modulus-porosity relation at room temperature with that at temperatures high enough so that "Mrozowski cracks," formed during cooling after graphitization, have been at least partially closed by thermal expansion.

Dynamic Young's modulus and thermal expansion have been measured as functions of temperature over the range 25 to 1800°C on specimens of POCO Grades AXF-5Q, AXM-5Q, and AXZ-9Q, each of which had previously been heat-treated by CMF-13 to 2900°C. (Room-temperature properties of these samples are listed in Table

XIII of Report No. 14 in this series.) The porosity of each sample as a function of temperature was calculated using single-crystal x-ray data from the literature to calculate carbon volume and dilatometric measurements to calculate bulk volume. These data were fitted, at a series of temperatures, to the equation

$$\frac{E}{E_0} \bigg|_T = 1 - k P_T$$

where E is Young's modulus in millions of psi, P is fractional porosity, and E_0 is Young's modulus for fully dense material -- determined by back-extrapolation of the line to zero porosity. Measurements on additional samples are needed, but preliminary results are listed in Table XX.

Between 25 and 1800°C, E_0 increased about 13%, with the greatest rate of change occurring in the 600-1200°C interval. The negative slope of the E vs P curve increased correspondingly, so that k in the above equation remained constant within about 1% over the entire temperature range.

The thermal expansions of all three samples were essentially identical, producing calculated porosity decreases averaging about 0.8% between 25 and 1800°C. This represents internal accommodation of some of the crystallite expansion, and should contribute to the increase in Young's modulus with temperature.

D. Thermal Expansion of POCO Graphites (P. Wagner)

Thermal expansion coefficients over the temperature range 25 to 645°C have been determined on 14 specimens of POCO graphite which had been heat-treated together in flowing helium to 2900°C. Densities of the various samples ranged from 1.539 to 1.904 g/cm³. Differences in thermal expansion behavior were small and unsystematic. When the expansion coefficients of all specimens were averaged, the standard deviation was 4.2%. It is estimated that the instrumental errors associated with the measurement are in the range 3 to 4%. In agreement with the results noted above in connection with Young's modulus measurements, it was concluded that, for this type of graphite, thermal expansion is essentially inde-

TABLE XX
ELASTIC PROPERTIES OF POCO GRAPHITES AT HIGH TEMPERATURES (PRELIMINARY)

Material	Property	Temperature, °C				
		25	600	900	1200	1800
Graphite	Carbon density, g/cm ³	2.2500 ^(a)	2.2135	2.1945	2.1754	2.1311
POCO AXF-5Q Sample 1	Porosity	0.1920	0.1889	0.18825	0.1876	0.1839
	Young's Modulus, 10 ⁶ psi	1.622	1.687	1.764	1.864	1.978
POCO AXM-5Q Sample 13	Porosity	0.2200	0.2166	0.2169	0.2158	0.2121
	Young's Modulus, 10 ⁶ psi	1.479	1.550	1.573	1.684	1.771
POCO AXZ-9Q Sample 15	Porosity	0.313	0.3096	0.30895	0.3083	0.3054
	Young's Modulus, 10 ⁶ psi	0.8905	0.9251	0.9688	1.0248	1.0983
Fully Dense Material (Extrapolated)	Young's Modulus, 10 ⁶ psi	2.947	2.947	3.012	3.218	3.329
	Slope, E vs P curve	-6.547	-6.547	-6.622	-7.125	-7.379
	k	-2.222	-2.222	-2.199	-2.214	-2.217

(a) Assumed room temperature value; all others are calculated from this value

pendent of bulk density. The internal accommodation which results in a decrease in fractional porosity as the graphite is heated probably occurs primarily within filler particles, where the void structure is unaffected by the variations in manufacturing procedure that alter bulk density.

VIII. LAW MATERIALS

A. Omnium Minier Natural Graphite Flour (J. A. O'Rourke, L. S. Levinson)

Through the European Representative of NASA, a sample of a very fine natural graphite flour has been received from Omnium Minier Societe Anonyme in Paris, France. The graphite is mined by Syndicat Lyonnais de Madagascar in Tananarive, Madagascar, and is purified and ground in LeHavre by Omnium Minier. The treatment is stated to involve, successively: physical and chemical processing to produce flake graphite with carbon content above 99.9%; crushing and micronizing to more than 80% finer than 7 μ ; purification to about 99.990% C.

The purity of the sample received by CMF-13 was verified only qualitatively, but appeared to be high. Electron microscopy showed the presence of fine flakes up to 20 μ long, with an average particle size less than 10 μ , as represented by Omnium Minier. Individual flakes had highly ordered, lamellar internal structures, typical of a well-organized natural graphite. X-ray measurements indicated an average crystallite thickness (L_c) of about 1000 Å and an interlayer spacing (d_{002}) of 3.354 Å, which is very near to that of a perfect graphite crystal.

IX. MANUFACTURING PROCEDURES

A. Effects of Temperature and Atmosphere During Curing and Baking (J. M. Dickinson, L. S. Levinson, R. D. Reiswig)

To investigate the effects of oxidation during the processing of an extruded, resin-bonded graphite, a series of samples has been intentionally exposed to air for 15-min periods at 200 to 700°C. The graphite used was extruded as 0.5-in. dia rod from a mix containing 85 parts

Great Lakes Grade 1008-S graphite flour, 15 parts Thermax carbon black, and 27 parts Varcum 8251 furfuryl alcohol resin binder catalyzed with 4% maleic anhydride. All samples were cured normally, in air, to 200°C. Lying on a bed of Thermax carbon black, they were then heated at 10°C/hr in argon to temperatures ranging from 200 to 700°C. As each selected temperature was reached, the furnace was flushed with air; the specimen was held in air at that temperature for 15 min; argon was reintroduced; and the specimen was furnace-cooled to room temperature.

Macroscopic examination revealed a roughening and darkening of the rod surfaces where they had been in contact with the supporting bed of carbon black. This is assumed to have been caused by gases evolved from the bed. The sample heated to 700°C also showed some roughening on the surface which was not in contact with the carbon black, presumably from oxidation.

No changes in microstructure were found in the interiors of the specimens which could be attributed to oxidation. Samples heat treated at 500°C or higher had roughened surfaces where the rod was in contact with the carbon black. Under this roughness, but not elsewhere, was a dark-etching zone 40 to 80 μ thick in which the hydrogen-ion etch appeared to have attacked the binder residue more actively than elsewhere in the structure, suggesting an effect of heteroatoms from the carbon black.

Colonies and stringers of voids were present in the samples after the 200°C curing treatment, with a few individual voids 25 to 50 μ dia. This void structure did not change significantly with heat-treatment to higher temperatures. Apparently most or all of the large voids found in a graphite of this type are formed by gas-entrapment either during mixing and extrusion or in the early stages of curing, while the binder is still plastic.

"C-face" cracks, formed at the interfaces between filler particles and binder residue, were not found in specimens heat-treated at or below 400°C and were present in specimens heat-treated at and above 500°C. Apparently microcracks of this type form as a result of binder shrinkage in the early stages of baking, soon after

binder pyrolysis has begun.

X. GRAPHITE PROPERTIES

A. Permeability of AAQ1 Graphite (P. Wagner)

Lot AAQ1 is an extruded, resin-bonded graphite made from 85 parts Great Lakes Grade 1008-S graphite flour, 15 parts Thermax carbon black, and 27 parts Varcum 8251 furfuryl alcohol resin catalyzed with maleic anhydride. Its bulk density is 1.90 g/cm³.

An attempt has been made to measure the permeability of AAQ1 graphite to gas flow, using a modified Ruska permeameter. This apparatus measures the rate of flow of nitrogen at room temperature through a disk of the material of interest, with a pressure drop of up to one atmosphere across the disk. By increasing the cross-sectional area and reducing the thickness of the sample, the sensitivity of the apparatus has been increased to the point where it can measure a permeability as low as 2×10^{-5} darcy. Permeability measurements on a group of commercial graphites gave values ranging from 0.012 darcy for ATJ graphite in the across-grain direction to above 0.3 darcy for some of the coarser-grained, lower-density graphites. These results were in reasonable agreement with permeability values found in the literature.

With AAQ1 graphite, the permeameter registered no gas flow for either with-grain or across-grain samples, indicating a permeability less than 2×10^{-5} darcy.

B. Crystalline Parameters of POCO Graphites (J. A. O'Rourke)

As has been discussed in several previous reports in this series, the effects of porosity on the properties of graphite are being investigated by measurements made on a group of POCO graphite samples each of which has been heat-treated in helium to 2900°C. Several additional samples have been added to this series, and are listed in Table XXI. As has previously been observed, the less-dense samples have the larger crystallite sizes.

TABLE XXI
CRYSTALLINE PARAMETERS OF POCO GRAPHITES

Specimen No.	Original POCO Grade	Heat- Treatment Condition	Crystalline Parameters	
			d_{002} , Å	L_c , Å
---	AXF	As-Received	3.375	280
---	AXF-QBG	As-Received	3.379	255
20	AXF-QB	Graphitized 2900°C	3.367	345
34	AXZ-9Q	Graphitized 2900°C	3.364	430
36	CZR-1	Graphitized 2900°C	3.363	445

XI. PUBLICATIONS RELATING TO CARBONS
AND GRAPHITES

- Dickinson, J. M. and Wewerka, E. M., "The Effects of Binder Viscosity and Molecular Size Distribution on the Fabrication and Physical Properties of Furfuryl Alcohol Resin Bonded Graphite", Carbon, Vol. 8, No. 3, p. 249-258, June, 1970.
- Green, W. V. and Zukas, E. G., "Le Graphite Emma-gasine Beaucoup D'Energie Lors D'un Fluage", translation by J. C. Festinger of paper titled "Stored Energy in Creep Deformed Graphite", Voici Des Idees, Mensuel Nos. 15-16, p. 78, Aout-Septembre, 1970.
- Green, W. V., Weertman, J. and Zukas, E. G., "High-Temperature Creep of Polycrystalline Graphite", Conference Preprints Book, 2nd International Conference on The Strength of Metals and Alloys, Asilomar Conference, p. 161-162, 30 August-4 September, 1970.
- Smith, M. C., "CMF-13 Research on Carbon and Graphite, Report No. 14, Summary of Progress from May 1 to July 31, 1970", LASL Report No. LA-4526-MS, October, 1970.
- Reiswig, R. D., "The Use of Hydrogen in Cathodic Vacuum Etching", Microstructures, 1, No. 2, p. 15-17, Oct./Nov., 1970.
- Wagner, P. and Dickinson, J. M., "Ambient and High Temperature Experiments on Boron-Doped Polycrystalline Graphites", Carbon, Vol. 8, p. 313-320, 1970.
- Green, W. V., Weertman, J. and Zukas, E. G., "High-Temperature Creep of Polycrystalline Graphite", Materials Science and Engineering, Vol. 6, p. 199-211, 1970.
- Gillis, P. P., Zukas, E. G. and Green, W. V., "Sub-grain Boundary Changes in Compression", Scripta Metallurgica, Vol. 4, p. 855-858, 1970.
- Armstrong, P. E., "Measurements of Elastic Constants", Chapter 8 in Techniques in Metals Research, Vol. 5, Part 2, Ed. R. F. Bunshah, Wiley, 1970.
- Dickinson, J. M. and Wewerka, E. M., "The Use of Gel Permeation Chromatography in the Development of High-Quality Graphite", Journal of Chromatography, Vol. 55, No. 1, p. 25-31, 1971.
- Baxman, H. R., Bertino, J. P., Bard, R. J., Hayter, S. W., O'Rourke, J. A. and Levinson, L. S., "Development of Particles Coated with Pyrolytic Carbon. IX. Studies of Commercial Experimental Coated Particles", LASL Report No. LA-4560, CONFIDENTIAL, 20 pgs., January, 1971.

McD/ga: 124(90)